Journal Pre-proof

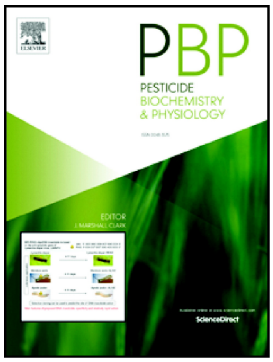

Molecular and genetic analysis of resistance to METI-I acaricides in Iranian populations of the citrus red mite Panonychus citri

Elaheh Shafiei Alavijeh, Jahangir Khajehali, Simon Snoeck, Rafaela Panteleri, Mohammad Ghadamyari, Wim Jonckheere, Sabina Bajda, Corinna Saalwaechter, Sven Geibel, Vassilis Douris, John Vontas, Thomas Van Leeuwen, Wannes Dermauw

PII: S0048-3575(19)30527-9

DOI: https://doi.org/10.1016/j.pestbp.2019.12.009

Reference: YPEST 4514

To appear in: *Pesticide Biochemistry and Physiology*

Received date: 12 October 2019

Revised date: 22 December 2019

Accepted date: 27 December 2019

Please cite this article as: E.S. Alavijeh, J. Khajehali, S. Snoeck, et al., Molecular and genetic analysis of resistance to METI-I acaricides in Iranian populations of the citrus red mite Panonychus citri, *Pesticide Biochemistry and Physiology* (2019), https://doi.org/10.1016/j.pestbp.2019.12.009

This is a PDF file of an article that has undergone enhancements after acceptance, such as the addition of a cover page and metadata, and formatting for readability, but it is not yet the definitive version of record. This version will undergo additional copyediting, typesetting and review before it is published in its final form, but we are providing this version to give early visibility of the article. Please note that, during the production process, errors may be discovered which could affect the content, and all legal disclaimers that apply to the journal pertain.

© 2019 Published by Elsevier.

Journal Pre-proof

Molecular and genetic analysis of resistance to METI-I acaricides in Iranian populations of the citrus red mite *Panonychus citri*

Elaheh Shafiei Alavijeh[a], Jahangir Khajehali[b,*], Simon Snoeck[c], Rafaela Panteleri[d,e], Mohammad Ghadamyari[a], Wim Jonckheere[c], Sabina Bajda[c], Corinna Saalwaechter[f], Sven Geibel[f], Vassilis Douris[e], John Vontas[e,g], Thomas Van Leeuwen[c,*], Wannes Dermauw[c,*]

[a]Department of Plant Protection, Faculty of Agriculture, University of Guilan, Rasht, Iran.

[b]Department of Plant Protection, College of Agriculture, Isfahan University of Technology, Isfahan 84156-83111, Iran.

[c]Laboratory of Agrozoology, Department of Plants and Crops, Faculty of Bioscience Engineering, Ghent University, Coupure links 653, 9000, Ghent, Belgium.

[d]Laboratory of Molecular Entomology, Department of Biology, University of Crete, GR-70013 Heraklion, Crete, Greece)

[e]Institute of Molecular Biology and Biotechnology (IMBB), Foundation for Research and Technology (FORTH), Nikolaou Plastira Street 100, 70013, Heraklion, Crete, Greece

[f]Bayer AG, CropScience Division, 40789 Monheim, Germany

[g]Pesticide Science Laboratory, department of Crop Science, Agricultural University of Athens, Iera Odos 75, 11855, Athens, Greece

*corresponding authors:

khajeali@cc.iut.ac.ir , thomas.vanleeuwen@ugent.be, wannes.dermauw@ugent.be

Journal Pre-proof

Abstract

The citrus red mite, *Panonychus citri*, is a major pest on citrus all around the world. Mitochondrial Electron Transport Inhibitors of complex I (METI-I) acaricides such as fenpyroximate have been used extensively to control *P. citri* populations, which resulted in multiple reports of METI-I resistant populations in the field. In this study, biochemical and molecular mechanisms of fenpyroximate resistance were investigated in *P. citri*. Seven populations were collected from Northern provinces of Iran. Resistance ratios were determined and reached up to 75-fold in comparison to a fenpyroximate susceptible population. Cross-resistance to two additional METI-I acaricides, pyridaben and tebufenpyrad, was detected. PBO synergism experiments, *in vivo* enzyme assays and gene expression analysis suggest a minor involvement of cytochrome P450 monooxygenases in fenpyroximate resistance, which is in contrast with many reported cases for the closely related *Tetranychus urticae*. Next, we determined the frequency of a well-known mutation in the target-site of METI-Is, the PSST subunit, associated with METI-I resistance. Indeed, the H92R substitution was detected in a highly fenpyroximate resistant *P. citri* population. Additionally, a new amino acid substitution at a conserved site in the PSST subunit was detected, A94V, with higher allele frequencies in a moderately resistant population. Marker-assisted back-crossing in a susceptible background confirmed the potential involvement of the newly discovered A94V mutation in fenpyroximate resistance. However, introduction of the A94V mutation in the PSST homologue of *D. melanogaster* using CRISPR-Cas9 did not result in fenpyroximate resistant flies. In addition, differences in binding curves between METI-Is and complex I measured directly, in isolated transgenic and wildtype mitochondria preparations, could not be found.

Key words: citrus red mite, fenpyroximate, METI-I, *Drosophila*, CRISPR-Cas9, target-site resistance

Journal Pre-proof

1. Introduction

Mitochondrial Electron Transport Inhibitors (METIs) inhibit electron transport in the mitochondrial respiratory chain and are commonly and successfully used against phytophagous mites like *Tetranychus urticae* Koch, *Panonychus ulmi* and *Panonychus citri* (McGregor) (Acari: Tetranychidae) (Hamaguchi et al., 1990; Konno et al., 1990; Van Leeuwen et al., 2015). METIs have been classified into groups depending on which of the four complexes (I-IV) of the electron transport chain they inhibit. METI-Is act on complex I (group 21, Insecticide Resistance Action Committee (IRAC) classification, Version 9.3, June 2019) (Hollingworth et al., 1994; Hollingworth and Ahammadsahib, 1995), the proton translocating NADH: ubiquinone oxidoreductase, the largest and most complex multi-subunit structure of the respiratory chain (Wirth et al., 2016). Complex I is responsible for catalyzing the electron transfer from NADH to coenzyme Q10 (ubiquinone). According to previous studies, ubiquinone and complex I inhibitors have at least partially overlapping binding sites (Degli Esposti, 1998), consisting of the PSST and the 49 kDa subunits (Lümmen, 1998; Schuler et al., 1999; Shiraishi et al., 2012). The PSST subunit is the most likely carrier of the iron-sulfur cluster N2 which couples the electron transfer to ubiquinone reduction (Duarte et al., 2002; Friedrich, 1998; Magnitsky et al., 2002).

The METI-I group includes the pesticide rotenone and the acaricides fenpyroximate, pyridaben, fenazaquin, pyrimidifen, tolfenpyrad and tebufenpyrad (Hollingworth et al., 1994; Hollingworth and Ahammadsahib, 1995). Because of their effectiveness against various mite species, METI-I acaricides were rapidly used globally (Devine et al., 2001). Unfortunately, the extensive use of this acaricide group resulted in wide-spread resistance (Van Leeuwen et al., 2015). In *T. urticae*, resistance to METI-I acaricides was initially associated with increased P450 activity based on synergism and enzyme activity tests (Devine et al., 2001; Herron and Rophail, 1998; Jum et al., 1995; Ozawa, 1994; Van Pottelberge et al., 2009), and P450 metabolic detoxification was suggested to be involved in cross-resistance between different compounds from the METI-I group (Kim et al., 2004; Stumpf and Nauen, 2001; Van Pottelberge et al., 2009). Subsequently, a genome-wide microarray revealed constitutively overexpressed P450s in *T. urticae* METI-I resistant strains. One of these P450s, CYP392A11, was functionally expressed and able to convert fenpyroximate to a non-toxic metabolite (Riga et al., 2015). However, CYP392A11 did not metabolize pyridaben or tebufenpyrad, suggesting that the P450 enzymes responsible for

METI-I metabolism may be compound specific. More recently, Bajda et al. (2017) reported the first METI-I target-site related mutation in the *T. urticae* PSST homologue of complex I (H92R substitution, *Yarrowia lipolytica* numbering). A back-crossing experiment validated the role of this target-site mutation in METI-I resistance, although it only explained a part of the total resistance phenotype (Bajda et al., 2017). The involvement of the latter mutation in resistance was further confirmed for fenpyroximate, pyridaben and tebufenpyrad in a QTL mapping approach using bulked segregant analysis (Snoeck et al., 2019).

The citrus red mite, *P. citri*, is one of the major cosmopolitan citrus pests (Gotoh et al., 2003; Pan et al., 2006; Vassiliou and Papadoulis, 2009), and is also a major pest in Iran (Jafari et al., 2016). Citrus red mites feed on the sap of leaves, fruits and green shoots of different citrus varieties, although the most severe damage is caused to the fruits (Jones and Parrella, 1984). The frequent use of pesticides, together with the high reproductive potential and short life cycle of *P. citri* facilitate resistance development in this species (Asano and Kamei, 1977; Ran et al., 2009; Yamamoto et al., 1995). METI-I compounds are an important tool in the management of citrus mites, and therefore the aim of this study was to investigate resistance levels to fenpyroximate in *P. citri*. Several populations were collected from citrus orchards in northern Iran and the role of detoxification as a resistance mechanism was analyzed by synergism experiments and biochemical assays. Genome-wide transcriptome profiling was used to identify genes involved in METI-I resistance in a subset of the populations. Finally, the role of a newly identified target-site (PSST) mutation in METI-I resistance was assessed by marker assisted back-crossing and CRISPR-Cas9 genome editing in *Drosophila*.

2. Materials and methods

2.1 Mite populations, and chemicals

In the spring and summer of 2016, *P. citri* populations were collected from citrus orchards of three Northern provinces of Iran, Guilan (Rasht, Rahimabad, Talesh, and Lahijan), Mazandaran (Ramsar and Sari) and Golestan (Gorgan) (Figure S1). Noteworthy, only fenpyroximate and pyridaben are registered for control of *P. citri* and *Phyllocoptruta oleivorai* (Acari: Acariformes: Eriophyoidea) in citrus orchards of northern Iran. Infested leaves were sampled randomly from

citrus trees and collected mites were reared in the laboratory on sour orange leaf discs (*Citrus aurantium* L.) at 25±2 ºC, 60±10% relative humidity (RH) with a 16:8 h (L:D) photoperiod. Commercial formulations of fenpyroximate 5% SC (Ortus®), pyridaben 20% SC (Sanmite®), tebufenpyrad 20% WP (Pyranica®), and cyenopyrafen 30% SC (Starmite®) were used in toxicity bioassays. All chemicals materials were of analytical grade and purchased from Merck (Darmstadt, Germany) and Sigma-Aldrich (Diegem, Belgium).

2.2 Adult bioassays, synergism assays, and cross-resistance screening

The resistance status of *P. citri* adult females was determined by the method of Tsagkarakou et al. (2009). Briefly, 10-20 female mites were put on the upper side of citrus leaf discs (9 cm^2) on wet cotton, which had been treated with different concentrations of fenpyroximate at 1 bar pressure in a Potter spray tower with 1.5 ml spray fluid (1.5 ± 0.05 mg spray fluid deposit/cm^2). The concentrations were selected based on preliminary bioassays. A control (distilled water) was also prepared. The plates were put in an incubator in controlled conditions at 25 ± 1°C, 60 % RH and 16:8 h (L:D) photoperiod. Each bioassay was replicated four times. Mortality was assessed 24 h after treatment. Mites that could walk normally after being touched with a camel's hair brush were scored as being alive. Resistance to other METI-I acaricides (pyridaben and tebufenpyrad) was assessed similarly while cyenopyrafen toxicity was only tested at a concentration of 0.1 and 1 mg a.i. L^{-1}. In order to evaluate synergistic effects, 4 h prior to fenpyroximate application, female mites were exposed to nontoxic concentrations of each synergist, 500, 300, and 300 mg L^{-1} of triphenyl phosphate (TPP), piperonyl butoxide (PBO), and diethyl maleate (DEM), respectively. Before use, PBO, DEM, and TPP were dissolved in acetone and diluted in distilled water. Mites sprayed with synergist only were used as the control. LC_{50} values, slopes, resistance ratios (RR), synergistic ratios (SR) and 95% confidence intervals were determined by probit analysis (POLO-Plus, LeOra Software, Berkeley, USA) (Robertson et al., 2017). The differences between LC_{50} values were supposed to be statistically significant when the 95% confidence intervals of the ratios did not include the value of 1.

2.3 Enzyme activity

Mass homogenates of freshly sampled mites were prepared by crushing 100 adult female mites in sodium phosphate buffer (0.1 M, pH 7.6; 350 µl) with a motorized Teflon pestle in glass tubes. The homogenate was centrifuged at 1000 *g* and 4 °C for 15 min. The resulting supernatant

was diluted to 200 µg protein ml^{-1} and used as an enzyme source. Protein concentration was measured by performing the Bradford assay (Bradford, 1976), using the commercially available coomassie protein assay kit (Perbio Science) and bovine serum albumin as a standard. The activity of esterases (Van Asperen, 1962), GSTs (Habig et al., 1974) and cytochrome P450 monooxygenases (P450s) (Van Leeuwen et al., 2005) was determined against the model substrates α- and β-naphthyl acetate (NA), 1-choloro-2,4-dinitrobenzene (CDNB) and 7-ethoxy-4-trifluoro methylcoumarin (7-EFC), respectively. Three to four replicates were conducted for all previously mentioned enzyme assays. SAS software was used to perform all statistical analyses ($p \leq 0.05$), means were compared with Tukey's test statistic (Rodemihouse et al., 2004).

2.4 RNA-seq

RNA-extraction of four *P. citri* populations (Rasht, Lahijan, Ramsar and Sari) was performed in Ghent, Belgium. Before RNA extraction, mites were grown on leaves of lemon (*Citrus limon* (L.) Osbeck) in controlled condition, 25 ± 1°C, 60 % RH and 16:8 h (L:D) photoperiod, for at least three generations (48 ± 4 days) and a toxicity test with fenpyroximate was performed to confirm the resistance status of each population. Total RNA was extracted from 100-130 adult female mites of each *P. citri* population using the RNEasy Plus mini kit (Qiagen, Belgium) with four-fold biological replication for each population. The quality and quantity of the total RNA was analyzed by a DeNovix DS-11 spectrophotometer (DeNovix, USA) and by running an aliquot on a 1% agarose gel. From the RNA samples, Illumina libraries were constructed with the TruSeq Stranded mRNA Library Preparation Kit with polyA selection (Illumina, USA). Resulting libraries were sequenced on an Illumina HiSeq 2500 and strand-specific paired reads (2 x 125bp) were generated (library construction and sequencing was performed at the Genomics Core Facility of the University of Utah, Utah, USA). Prior to read-mapping, the quality of the reads was verified using FASTQC version 0.11.5 (Andrews, 2010). One replicate (replicate 2) of the Rasht population failed to pass the quality control (failure for both "per sequence GC content" and "overrepresented sequences") and was excluded from further analyses.

2.5 *De novo* transcriptome assembly and transcript annotation

For each *P. citri* population a *de novo* transcriptome assembly was created using CLC Genomics Workbench 11 using a random selection of 10 million reads per replicate per population (for the *de novo* transcriptome assembly of the Rasht population, replicate 2 was not included (see

above) and 13.33 million random reads were used per replicate per population for the Rasht *de novo* assembly). Next, resulting assemblies were merged and long open reading frames (ORFs) of each transcript were extracted using Transdecoder v. 5.2.0 (Haas et al., 2013) with a minimum ORF length of 100 amino acids. Next, extracted ORFs were filtered using CD-HIT-EST (Li and Godzik, 2006) with an identity threshold of 98% (-c 0.98) and a word size of 10 (-n 10). Those transcripts to which the filtered ORFs belonged (from here on named "merged assembly") were used for further analysis (see below). The overall mapping success rate against the merged assembly was used as a measure for assembly quality. The *P. citri* transcript encoding the PSST subunit of complex I (see Introduction) was identified based on a tBLASTn search using the *T. urticae* PSST subunit (tetur07g05240) as query. Furthermore, all transcripts of the final assembly were loaded into OmicsBox 1.1.78 and used as query in a BLASTx 2.9.0+ search, using an E-value threshold of E^{-3} and the "fast" setting (Shiryev et al., 2007), against the NCBI non-redundant (nr) protein database (version of 20th February 2019). Blast2GO was subsequently used to map and annotate gene ontology (GO) terms to transcripts based on the sequence hits retrieved by the BLASTx search (Götz et al., 2008). Finally, the InterProScan pipeline (Finn et al., 2016) was run and InterPro identified GO terms were merged to the Blast2GO annotated GO terms.

2.6 Expression quantification and principal component analysis (PCA)

Before read alignment, those transcripts that had a BLASTx hit with either *Citrus* sp. or viruses were excluded from the final assembly. Paired-end sequences were pseudoaligned with kallisto (100 bootstraps) to create abundance-estimates (Bray et al., 2016). Differential expression analyses were performed with sleuth 0.29.0 running on R 3.4.4 according to sleuth default settings, and by using the following R-packages; biomaRt 2.34.2, edgeR 3.20.9, limma 3.43.9, dplyr 0.7.6 and bindrcpp 0.2.2. The Wald test in sleuth was used to analyze the kallisto bootstrap estimates (Pimentel et al., 2017) while the transformation function $\log_2(x + 0.5)$ (Sahraeian et al., 2017) option in the sleuth_prep command was used to calculate the effect size (β value) as $\log_2$-based fold changes. Transcripts with a $|\log_2 FC| \geq 1$ and q-value (Benjamini-Hochberg multiple testing corrected *p*-value) ≤ 0.05 between the susceptible (Rasht) and one of the resistant (Lahijan, Ramsar and Sari) *P. citri* populations were considered as differentially expressed. For the differentially expressed transcripts (DETs) of each comparison a GO enrichment analysis

was performed using the Bioconductor package GOSeq (version 1.24.0) (Young et al., 2010). The resulting *p*-values from GOSeq were corrected using the Benjamini-Hochberg method (Benjamini and Hochberg, 1995) and only those GO categories with an adjusted *p*-value of less than 0.05 were considered significantly enriched. Finally, a PCA was created using the R-packages sleuth, dplyr 0.7.6 and ggplot2 3.0.0.

2.7 cDNA synthesis and RT-qPCR

A set of DETs between two *P. citri* populations (Rasht and Sari) was evaluated by RT-qPCR. Gene specific primers were designed using Primer3 v.0.4.0.0 (Rozen and Skaletsky, 2000). The RT-qPCR primers used, including the primers for the genes of interest, as well as those for the two reference genes (*GAPDH and ELF1a*, Niu et al., 2012), can be found in Table S4. Total RNA was extracted as described above, and 2 µg of total RNA was used as template for synthesizing cDNA with the Maxima First Strand cDNA synthesis Kit for RT-qPCR (Fermentas Life Sciences, Aalst, Belgium). Three biological and two technical replicates were used and non-template controls were added to exclude sample contamination. The RT-qPCR analysis was performed on a Mx3005P qPCR thermal cycler (Stratagene, Agilent Technologies, Diegem, Belgium) with Maxima SYBR Green qPCR Master Mix (2x) and ROX solution (Fermentas Life Sciences) according to the manufacturer's instructions. The run conditions of the RT-qPCR were as follows: 95 °C for 10 min followed by 35 cycles of 95 °C for 15 s, 55 °C for 30 s and 72 °C for 30 s. Finally, a melting curve was generated (from 65 °C to 95 °C, 1 °C per 2 s), to confirm the presence of a single amplicon. The standard curve and amplification efficiencies of each primer pair were detected using fourfold dilution series of pooled cDNA. The resulting amplification efficiencies were incorporated in the calculations of the expression values. Relative expression levels and significant gene expression differences (one-sided unpaired t-test) were calculated using qbase + version 3.0 (Hellemans et al., 2007).

2.8 Single mite DNA preparation and amplification of PSST fragment

To perform DNA extraction on single *P. citri* males, individual males were homogenized in 20 µl STE buffer (100 mM NaCl, 10 mM Tris-HCl, and 1 mM EDTA) with 2 µl (10 mg/ml) proteinase K (Sigma-Aldrich). Homogenate was incubated at 60 °C for 30 min followed by proteinase K inactivation for 5 min at 95 °C. After cooling, homogenate was directly used in a PCR reaction. (see Table S5 for PCR conditions). PCR primers were designed based on

Rasht_contig_1338, encoding a *P. citri* PSST fragment (see Table S4 for primer sequences). Resulting DNA was Sanger sequenced by LGC Genomics (Germany), and analysed using BioEdit 7.0.1 software (Hall, 1999). For each *P. citri* population (Rasht, Lahijan, Ramsar and Sari), the PSST fragment of 20 single males was amplified and sequenced.

2.9 Introgression of the A94V PSST mutation into a susceptible background

Introgression by marker assisted selection was performed as previously described by Bajda et al. (2017). Briefly, a virgin female of the Rasht population (susceptible to fenpyroximate, genotype A94/A94 for PSST) was crossed with a haploid male of the Lahijan population (fenpyroximate resistant, genotype V94/V94 for PSST), in two biological replicates. The heterozygous virgin females (genotype A94/V94) were crossed with Rasht males (A94 genotype). After they had laid enough eggs, presence of the target-site mutation was determined in the heterozygous F1 females with PCR-RFLP using a TseI restriction site (New England BioLabs® Inc.) (Table S4 and Table S5). The back-cross was repeated for six generations and in the last generation, heterozygous females were crossed with their sons which had either the genotype A94 or V94; resulting in homozygote lines with genotypes A94/A94 (S-line) and V94/V94 (R-lines). Fenpyroximate toxicity to S and R-lines was assessed as above.

2.10 CRISPR-Cas9 genome editing in *Drosophila*

2.10.1 Strategy for genome editing

An *ad hoc* CRISPR-Cas9 strategy was implemented in order to generate *Drosophila* strains bearing mutation A94V (*Yarrowia lipolytica* numbering, corresponding to A105V in *Drosophila* PSST and corresponding to A112V in *T. urticae* PSST) at the PSST (ND20) gene, similar to the one used in Bajda et al. (2017). Two CRISPR targets, sgRNA1 and sgRNA2 were used (Figure S2) as previously described (Bajda et al., 2017) and the same sgRNA expressing plasmids were employed. A double stranded donor plasmid (File S1, insert size 2183bp), was synthesized *de novo* (GenScript, USA) to facilitate homologous recombination, containing two homology arms of circa 950 bp length spanning the 286 bp target region that contains the A105V (GCT->GTT; A94V in *Y. lipolytica*) mutation as well as certain additional synonymous mutations (Figure S2) serving either as molecular markers (to facilitate molecular screening of CRISPR events), or to prevent unwanted CRISPR digestion

of the donor. These include a mutation resulting in the abolishment of a Tsp45I restriction site, as well as the introduction of a SgrBI site in genome modified alleles (Figure S2).

2.10.2 Molecular screening and establishment of genome modified lines.

nos.Cas9 pre-blastoderm embryos were injected with a mix containing 75 ng/μl of each sgRNA plasmid vector and 100ng/μl of donor template. Hatched larvae were transferred into standard fly artificial diet and after 9-13 days surviving G_0 adults were collected and individually backcrossed with nos.Cas9 flies. In order to screen for CRISPR events, G_1 generation progeny from each cross were initially screened *en masse* followed by individual crosses as previously described (Bajda et al., 2017; Douris et al., 2016). DNA pools from c. 30 individuals or individual flies were used for amplification with specific primers CG9172_dia_F/R (Table S4) that were designed accounting for the synonymous mutations introduced in the relevant target sequences in order to generate a 294 bp diagnostic fragment that is specific to genome modified alleles, but not wild-type ones (Figure S3A). PCR was performed with Kapa Taq polymerase as previously described (Bajda et al., 2017) using ~60 ng of digested template DNA mix. An alternative strategy was also used, which consisted of PCR amplification with a "generic" primer pair CG9172_ver F/R (Table S4) which was designed to amplify a 559 bp fragment that may be derived by either wild type or genome modified alleles. Following PCR amplification, the product was digested with the diagnostic enzyme SgrBI introduced in the donor plasmid sequence, producing two diagnostic fragments of 328 and 231 bp (Figure S3B). Crosses that proved positive for genome modified alleles were further explored to identify individual flies bearing mutant alleles and to establish homozygous lines (see Figure S4 for the whole crossing scheme). DNA was extracted from several homozygous female and hemizygous male adults, amplified by using primers CG9172F/R or CG9172_ver F/R (Table S4), and the relevant amplification fragments were sequence verified (Cemia, Larissa, Greece) for the presence of the desired mutations (Figure S3C).

2.10.3 Toxicity bioassays with Drosophila **nos.Cas9** *or PSST A94V mutant*

Tebufenpyrad, pyridaben and fenpyroximate of technical grade were purchased from Sigma Aldrich (Darmstadt, Germany) and used in contact assays and/or topical applications with *Drosophila* flies. Contact assays were performed as described previously (Samantsidis et al.,

2019). More specifically, 10 adult female flies (1 to 3-days old) were used in each toxicity assay. Flies were collected in plastic vials and transferred in scintillation vials coated with insecticide. Serial dilutions of 6 to 7 concentrations of technical grade METIs in acetone were used for dose response bioassays, while vials coated only with acetone served as control. The vials were plugged with cotton that was kept moist with 5% sucrose solution. Each METI bioassay was tested in 3 replicates. Mortality was scored after 24 h.

Topical application of fenpyroximate was performed on 1 to 3-days old female flies. Fenpyroximate was dissolved in acetone and serial dilutions were used to generate the appropriate concentrations. Each dose was applied as a volume of 1 µl per fly using a 10 µl Hamilton syringe. Flies were immobilized by keeping them on an ice-cold slide. For each concentration 40-45 flies were tested. Following insecticide application, the flies were transferred in glass scintillation vials covered with cotton moisturized with 5% sucrose solution. The vials were maintained in a 25°C incubator while mortality was scored after 24 h.

2.11.4 NADH:ubiquinone oxidoreductase activity measurements and ligand pIC50 determination

Mitochondria of either the nos.Cas9 or A94V mutant fly line were isolated from the thoracic flight muscles of 5-7 day old flies by a modification of the procedure described by Wood and Nordin (1980). Briefly, thoraces were excised from approximately 150 adult female flies and homogenized with a Teflon pestle in 3 ml chilled buffer I (154 mM KCl, 1 mM EDTA, pH adjusted to 7.2 with KOH, Halt Protease Inhibitor Cocktail (100X) - Thermo Fisher Scientific). Cooled homogenate was centrifuged twice at 500g followed by syringe filtration through 8 layers of a sterile gauze. Flow-through was centrifuged once at 5000g for 10 min. The resulting pellet was washed once in 800 µl of buffer I. Mitochondria were pelleted at 5000 g for 10 min and resuspended in 100 µl of buffer II (200 ml Mannitol, 50 mM Sucrose, 1 mM EDTA, in 10 mM HEPES, adjusted with NaOH to pH 7.2). Mitochondria isolation was performed in triplicate per line. One out of three A94V mutant fly lines was selected to perform the mitochondrial extractions.

For measurement of NADH:ubiquinone oxidoreductase activity, a combined assay for NADH:ubiquinone oxidoreductase and ubiquinol:cytochrome-c-oxidoreductase activity using

reduced ß-NADH (TCN Biochemicals) as substrate and monitoring the reduction of cytochrome c by following the increase in optical density at 550 nm was used as published previously (Hatefi and Stiggall, 1978). In brief, cytochrome c from equine heart (Sigma, C2506) was mixed with NADH and a sodium cyanide solution for final concentrations of 0.93 mg/ml, 40 µM and 61 µg/ml respectively. Sodium cyanide prevented reduced cytochrome c from being oxidized by cytochrome c:02-oxidoreductase also present in mitochondria. 25 µl of this cytochrome c solution was added to 25 µl mitochondrial protein/inhibitor solution. This protein/inhibitor solution contained material for final concentrations of 1.25 mg/ml CHAPS (Sigma C3023) and 125 mM KCl (Merck 1.04936.1000) dissolved in potassium buffer pH 7.2 c(PO4)=50 mmol/L as well as the investigated inhibitors as applicable.

All assays including enzyme activity measurements and IC_{50} determinations were performed in a final volume of 50 µl containing inhibitor stocks dissolved in DMSO with a final DMSO concentration of 0.1%. The concentration range of inhibitors was 0.64 pM – 10 µM. Each concentration was tested in two technical replicates and 2-3 biological replicates. The enzyme activity was calculated based on two control reactions (no inhibitors and 100 nM fenazaquin in DMSO). As enzyme activity varies by each isolation of mitochondria, the amount of mitochondria used in each reaction was adjusted to be in line with the requirements of the activity assay. All enzyme activity measurements and IC_{50} determinations were carried out in 384-well plates (384 flat bottom transparent, Greiner) using a TECAN Infinity multimode microplate reader (Tecan Group Limited., Switzerland). pIC50 values (= negative logarithm of IC_{50}) were calculated using the R-package *drc* (Ritz et al., 2015). A four-parameter logistic curve (LL.4) was fitted to the dose-response (% inhibition relative to inhibition by 100 nM fenazaquin) data using the *drm* function within the *drc* package and statistical difference between pIC_{50}s of METI-Is was determined by means of a *t*-test using the *compParm* function within *drc*.

3. Results

3.1 METI resistance levels and detoxification enzyme activities in *P. citri* populations from Iran

Fenpyroximate toxicity was assessed in seven *P. citri* populations (Table 1). Fenpyroximate was the most toxic (lowest LC_{50}) for the Rasht population and, hence, this population was considered

as the susceptible population. Relative to the Rasht population, the highest resistance ratios (RRs) were found for the Ramsar and Sari populations (>76.1 fold) while moderate RRs were determined for the Rahimabad, Gorgan, Talesh and Lahijan populations (7.0, 7.3, 19.8 and 19.9 fold, respectively). TPP significantly synergized fenpyroximate toxicity for the Gorgan, Talesh, Rahimabad and Lahijan population, while DEM only significantly synergized fenpyroximate toxicity for the Talesh and Rahimabad population. However, low synergism ratios (SRs) were observed for both TPP (1.3-3.0 fold) and DEM (1.0-1.7 fold). PBO, on the other hand, significantly reduced the toxicity of fenpyroximate in all tested populations and PBO SRs were higher (3.0-6.3 fold) than those determined for TPP and DEM. Across all *P. citri* populations, the Rahimabad population had the highest SR for both DEM, TPP and PBO. PBO SRs could not be determined for the Ramsar and Sari population since LC_{50}s were higher than 500 mg/L, the upper limit of our toxicity assay. The Sari population also showed high levels of resistance to pyridaben and tebufenpyrad, relative to the susceptible Rasht population (RR: 31.725 and 259.250 fold, respectively) (Table 2). Lahijan and Ramsar also showed moderate resistance for tebufenpyrad (RR: 18.967 and 23.490). For cyenopyrafen, LC_{50}s were not determined but 100% mortality was observed at a concentration of 0.1 and 1 mg a.i. L^{-1} for the Rasht, Lahijan, Ramsar and Sari population.

The *in vitro* activities of CCEs, GSTs and P450s were determined on whole mite homogenates of *P. citri* populations and are presented in Table 3. Esterase (α-NA) and GST activities were significantly higher in the Gorgan and Talesh population compared to the Rasht population, with a 6.155- fold and 2.196- fold increase in esterase (α-NA) and GST activity, respectively, in the Gorgan population. Of the four METI-I resistant populations examined, only the Lahijan population had a P450 activity that was significantly higher (1.6-fold) than the susceptible Rasht population.

3.2 *de novo* assembly, *RNA* sequencing, PCA and differential transcript expression analysis

Illumina sequencing generated approximately 53,074-72,328 million strand-specific, paired-end reads per population. Reads of each population are available in the Gene-Expression Omnibus (GEO) repository with accession number GSE142139. The final *de novo* assembly consisted of 17,784 transcripts (File S2) and was generated by merging the *de novo* transcriptome assembly of each population (File S3) followed by the removal of redundant transcripts. The N50 for the

merged transcripts was 2,378 bp and the average pseudoalignment mapping rate of reads against the 17,784 transcripts was 90% ± 1.1 STD, consistent with a high-quality transcriptome assembly (Table S1). A Blast2GO analysis revealed that 15,508 of the 17,784 transcripts had a BLASTx hit (Table S2) and 102 transcripts were either viral or from *Citrus* sp. (Table S3). These 102 transcripts were removed from further analyses. Next, reads were pseudoaligned against the 17,682 non-viral/non-citrus transcripts (see Supplementary File of GEO accession GSE142139) using kallisto. A principal component analysis (PCA) across all RNAseq samples revealed that 45.86% of the total variation could be explained by PC1 while 30.15% could be explained by PC2 (Figure 1). RNAseq replicates clustered by population, confirming sample quality. We used sleuth to perform a differential transcript expression analysis ($|\log_2 FC| \geq 1$, q-value ≤ 0.05). Transcript expression levels were pairwise compared between each resistant mite population (Lahijan, Ramsar and Sari) and the susceptible (Rasht) population.

The Sari population differed the most from the susceptible Rasht population and had 904 DETs, whereas the Ramsar and Lahijan population only had 520 and 414 DETs, respectively. For a subset of transcripts, differential expression was validated independently by RT-qPCR (Figure S5). As shown in Figure 1C, the majority of DETs were not shared between the three comparisons, but 331 DETs (36.6% and 63.6% of the total number of DETs of Sari and Ramsar, respectively) were shared between the Ramsar and Sari populations (Table S6 and Table S7). In contrast, the majority of differentially expressed transcripts were population-specific for Lahijan. These findings align with the PCA results, with Sari and Ramsar clustering on PC2 away from Lahijan (Figure 1B). A GO enrichment analysis revealed that among the DETs between the Lahijan and Rasht populations five GO terms were significantly enriched, including "positive regulation of translational elongation/termination" (GO0045901, GO0045905) and "translational frameshifting" (G0006452) (Table S8), while among the DETs of the other comparisons no significantly enriched GO-terms were found. Only a few P450 transcripts were differentially expressed in the resistant *P. citri* populations, with fold changes being modest overall. Ramsar (three overexpressed contigs, $\log_2 FC$ 1.1-1.6) and Sari (six overexpressed contigs, $\log_2 FC$ 1.2-3.9) shared one overexpressed P450 contig (Lahi_contig_11061) while Lahijan had only one uniquely overexpressed P450 (Rasht_contig_4055, $\log_2 FC$ of 1.1) (Table S7). Ramsar_contig_7025 encodes a NFU1 iron-cluster scaffold protein and was one of the most highly overexpressed transcripts (> 60-fold) in both Sari and Ramsar, while

Ramsar_contig_3746 and Rasht_contig_6350, encoding the NADH dehydrogenase [ubiquinone] iron-sulfur protein 4 (orthologous to human NDUFS4) and the iron-sulfur cluster assembly 2 protein (orthologous to human ISCA2), respectively, where 5 and 2-fold overexpressed in these strains (Table S7). Finally, Sari_contig_3709 was about 6-fold overexpressed in both Sari and Ramsar and encodes the beta subunit of the mitochondrial NAD+ dependent isocitrate dehydrogenase (orthologous to human IDH3B), an enzyme of the tricarboxylic acid cycle, while a metal regulatory transcription factor 1 (MTF-1) encoding transcript (Rasht_contig_582) was underexpressed in both Ramsar and Sari (Table S6 and Table S7).

3.3 Presence of PSST mutations in *P. citri* populations

A PSST fragment from 20 single males of the Rasht, Lahijan, Ramsar and Sari population was PCR amplified and analyzed for the presence of the previously reported H92R mutation (Bajda et al., 2017). The mutation was observed in some populations. Males of the Sari population had the highest frequency of the H92R mutation (35%), while the frequency was 5%, 10% and 10% for males of Rasht, Lahijan and Ramsar populations, respectively. In addition, we identified a previously unreported PSST mutation, A94V. The A94V mutation was found in one Rasht male, while 55% of the Lahijan males harbored the A94V mutation (Figure 2).

3.5 Marker-assisted back-crossing of PSST A94V into a susceptible *P. citri* background.

The marker-assisted back-crossing experiments successfully generated two independent lines with the A94V substitution fixed in the susceptible background of the Rasht population. The fenpyroximate and pyridaben toxicity profile for the parental and back-crossed *P. citri* populations are reported in Table 4. The two introgressed replicate lines S1 and S2, without the A94V mutation, had fenpyroximate RRs of 0.71 and 0.82 compared to the susceptible Rasht population. In contrast, the two introgressed replicate lines R1 and R2, with the A94V mutation, had fenpyroximate RRs of 9.17 and 10.68, respectively, compared to the susceptible Rasht population. The RRs for pyridaben (1.7 and 1.4 for R1 and R2, respectively) were less pronounced (Table 4).

3.6 Introduction of A94V in the PSST homologue of *Drosophila* by CRISPR-Cas9 followed by homologous recombination-directed gene modification (HDR)

The A94V mutation (*Y. lipolytica* numbering, A105V *Drosophila* numbering) was introduced in *Drosophila* via CRISPR/Cas9 coupled with Homologous Directed Repair (HDR) as described in Materials and Methods. Following injection of nos.Cas9 embryos, 46 adult (G_0) flies were backcrossed with nos.Cas9 flies and generated viable progeny (G_1). Samples from these G_1 flies were screened and 4 were found to be positive for HDR (Figure S3). These lines were crossed to balancer stocks as shown in Figure S4 and three of them generated homozygous lines bearing the A94V sequence at the target gene (Figure S3C). Contact and topical bioassays were used to investigate the toxicity of METI-I acaricides to *Drosophila* nos.Cas9 and the three A94V lines. Contact assays revealed that at 10, 100 or 1000 mg/L pyridaben fly mortality was significantly lower in the nos.Cas9 line compared to the A94V lines. Similarly, at 1000 mg/L tebufenpyrad, fly mortality was lower in the nos.Cas9 line compared to the A94V lines, albeit not significantly (p value= 0.0722). On the other hand, 5,000 mg/L fenpyroximate was not toxic to *Drosophila* in contact assays (Figure S6). Topical assays with fenpyroximate, on the other hand, showed fly mortality at 1,000, 2,500 and 5,000 ppm fenpyroximate but no significant differences could be observed between the mean mortality of nos.Cas9 and A94V fly lines (Figure 3).

3.7 *NADH:ubiquinone oxidoreductase activity measurements and ligand pIC_{50} determination*

The inhibition curves of tebufenpyrad, fenpyroximate and pyridaben for complex I of mitochondria prepared from nos.Cas9 and A94V *Drosophila* lines are shown in Figure 4. The pIC_{50} values (95% CI) of tebufenpyad, fenpyroximate and pyridaben were 8.87 (8.78-8.96), 8.15 (8.05-8.26) and 8.48 (8.35-8.61) for the nos.Cas9 line, respectively, and 8.90 (8.81-8.98), 8.26 (8.16-8.36) and 8.46 (8.32-8.61) for the A94V line, respectively. The pIC_{50} values of tebufenpyrad, fenpyroximate and pyridaben were similar (nanomolar range) to a previously reported pIC_{50} value of pyridaben for complex I from rat liver mitochondria (Hollingworth et al., 1994). No significant differences were found between METI-I acaricide pIC_{50} values of the nos.Cas9 line and those of the A94V line.

4. Discussion

According to the Arthropod Resistance Pesticide Database, 74 resistance cases to 28 different acaricides have been reported for *P. citri*, including the METI-I pesticide pyridaben (Mota-Sanchez and Wise., 2019). Resistance to, and cross-resistance between, METI-I group acaricides has been reported from the mid-1990s in spider mites (Van Leeuwen et al., 2009). Although METI-I resistance is well studied for *T. urticae* and *P. ulmi*, knowledge on incidence and mechanisms of METI-I resistance is far more limited for *P. citri*. In this study, we characterized fenpyroximate resistance in seven *P. citri* populations from Iran. The lowest fenpyroximate LC_{50} (6.57 mg/L) was found for the Rasht population (Table 1) and was similar to the LC_{50} typically found for susceptible *T. urticae* strains determined with the same methods (Van Pottelberge et al., 2009). Other sampled *P. citri* populations showed low to high fenpyroximate resistance ratios (RRs) compared to the Rasht population. The highest fenpyroximate RR was found for the Sari population (RR > 76 fold) and was considerably higher than those reported for *Panonychus* sp. in previous studies (Kumral and Kovanci, 2007; Nauen et al., 2001), but lower than those reported for *T. urticae* (> 500-fold, Nauen et al., 2001; Stumpf and Nauen, 2001; Van Pottelberge et al., 2009). For four populations we also examined resistance to two other METI-I acaricides, tebufenpyrad and pyridaben, and a METI-II acaricide, cyenopyrafen. The *P. citri* Sari population showed high levels of resistance to pyridaben and tebufenpyrad, while the Lahijan and Ramsar populations showed moderate resistance only to tebufenpyrad (Table 2). METI-I cross-resistance has been reported numerously for tetranychid species (see Kim et al., 2004; Stumpf and Nauen, 2001; Van Pottelberge et al., 2009), and since tebufenpyrad and pyridaben are not registered or rarely used in citrus orchards in Iran (Nourbakhsh, 2018), this strongly suggests that there is moderate to high level of cross-resistance between fenpyroximate and other METI-I acaricides in the fenpyroximate resistant *P. citri* strains of this study. Cross-resistance between pyridaben (METI-I) and cyenopyrafen (METI-II), on the other hand, has only been recently reported for *T. urticae* (Khalighi et al., 2016; Sugimoto and Osakabe, 2014), and such cross-resistance was not observed for the resistant *P. citri* populations in this study.

Low levels of synergism were observed following pre-treatment of fenpyroximate-sprayed mites with either TPP or DEM in the *P. citri* populations of this study. Overall, this is in line with the *in vitro* determined activities of detoxification enzymes that are blocked by these synergists, with elevated CCE and GST activities observed only for the Gorgan and Talesh populations, which showed only limited levels of fenpyroximate resistance (Table 1, Table 3). PBO significantly

synergized fenpyroximate toxicity in the resistant *P. citri* populations but, to a similar extent, also in the susceptible Rasht population, suggesting that P450s do not play a major role in fenpyroximate resistance in these resistant *P. citri* populations. PBO SRs could not be determined for the highly fenpyroximate resistant *P. citri* populations Sari and Ramsar. However, as we only observed elevated P450 enzyme activity in the Lahijan population (Table 3) and not in the Sari or Ramsar populations, P450s likely do not play a major role in fenpyroximate resistance in the latter populations. For *T. urticae*, the effect of PBO on fenpyroximate toxicity has often been found to be high (Ay and Kara, 2011; Kim et al., 2004; Van Pottelberge et al., 2009). In addition, Riga et al. (2015) showed that fenpyroximate could be metabolized *in vitro* by a recombinant *T. urticae* P450 (CYP392A11), and transgenic *Drosophila* flies ectopically expressing CYP392A11 showed threefold resistance to fenpyroximate. However, the *in vivo* role of this P450 in fenpyroximate resistance in *T. urticae* has still not been demonstrated.

To identify putative players in fenpyroximate resistance on a genome wide scale, we performed a differential expression analysis between a selection of fenpyroximate resistant *P. citri* populations (Lahijan, Sari and Ramsar) and a susceptible population (Rasht). In line with the results from the PBO synergism experiments and P450 enzyme activity measurements, we found few P450 transcripts among the DETs. Among the DETs shared between the two most resistant populations (Sari and Ramsar), some may play a role in fenpyroximate resistance (Table S6, Table S7). The NFU1 homolog in bacteria (NfuA) is known to be crucial for complex I stability (Bandyopadhyay et al., 2008) and for protection against oxidative stress (Burschel et al., 2019; Melber et al., 2016; Zimbler et al., 2012) while ISCA2 and NDUFS4 mutants in humans were shown to have severely reduced complex I activity (Al-Hassnan et al., 2015; Budde et al., 2000; Petruzzella et al., 2001; Sheftel et al., 2012). Their overexpression in Ramsar and Sari might be a "compensation mechanism" for fenpyroximate inhibition of complex I and the resulting oxidative stress, the latter being the primary mechanism of METI-I toxicity (Sherer et al., 2007). Mitochondrial NAD+ dependent isocitrate dehydrogenase is located in close vicinity of complex I (Porpaczy et al., 1987) and generates NADH, which is used by complex I to drive electron transport (Al-Khallaf, 2017; Larosa and Remacle, 2018). The overexpression of its encoding transcript in fenpyroximate resistant *P. citri* populations seems counterintuitive as it was shown that a high NADH/NAD^+-ratio drives reactive oxygen species production (Korge et al., 2016).

Similarly, we also observed underexpression of an MTF-1 encoding transcript. This observation contradicts earlier findings that indicated that overexpression of MTF-1 confers resistance against oxidative stress (Bahadorani et al., 2010; Saini et al., 2011).

In the closely related *T. urticae*, METI-I-resistance is a complex mechanism, including both detoxification by P450s and target-site resistance conferred by H92R in the PSST subunit of complex I (Bajda et al., 2017; Snoeck et al., 2019). In the PSST transcript of the Sari population we identified an identical mutation and subsequently monitored the presence of this mutation in 20 single males of the Rasht, Lahijan, Sari and Ramsar population. We found that the PSST H92R mutation was segregating in all *P. citri* populations, but that the Sari population, the only population that was resistant to all three tested METI-I acaricides (Table 1, Table 2) had the highest H92R allele frequency (35%). The association of the PSST H92R mutation with METI-I resistance in *P. citri*, which belongs to the same subfamily as *T. urticae* (Tetranychinae), provides a new example of parallel evolution and further supports the role of this mutation in METI-I resistance. Additionally, in the PSST subunit of the Lahijan population we identified a new mutation, A94V, located two amino acids away from the H92R mutation. Like H92, A94 belongs to a PSST fragment that was photoaffinity labeled by a photoreactive derivative of fenpyroximate (Shiraishi et al., 2012, Figure 2A - residues of *B. taurus* PSST in grey font). A PROVEAN (PROtein Variation Effect ANalyzer) analysis also predicted that a mutation to valine at this position is deleterious (PROVEAN score -3.752, Choi and Chan, 2015). Because of its closely adjacent proximity to the H92R mutation and the predicted deleterious effect, we investigated the frequency of the A94V mutations in single males of the Rasht, Lahijan, Ramsar and Sari populations. The A94V mutation was found in only one male of the Rasht population, was absent in the Sari and Ramsar populations, but is present in more than half of the males of the moderately resistant Lahijan population (Figure 2B), suggesting a possible association with moderate resistance against fenpyroximate. Similar as in Bajda *et al.* 2017, the role of this mutation in METI-I resistance was further investigated by marker-assisted back-crossing between a resistant (Lahijan) and a susceptible (Rasht) population. In this way, we aimed to uncouple the mutation from other resistance conferring genes by reducing the genetic background of the resistant parent to a minimum (Hospital, 2005). Remaining fenpyroximate resistance levels were about 10-fold compared to the susceptible Rasht population (Table 4), while pyridaben resistance levels were less than 2-fold. As the moderately resistant phenotype of

the Lahijan population could not be completely explained by the A94V mutation, this might suggest that multiple factors play a role in resistance of the Lahijan population against fenpyroximate.

Back-crossing reduces the proportion of donor genome by 50% each generation, except on the chromosome carrying the characteristic, which will have a slower rate of decrease as a result of linkage drag (Naveira and Barbadilla, 1992). Therefore, to further test the possibility that A94V is involved in resistance, we used CRISPR-Cas9 technology to introduce the mutation in the PSST homologue of *D. melanogaster*. CRISPR-Cas9 modified *Drosophila* A94V lines were successfully created. Of particular note, complex I activity in a PSST S94A mutant of *Y. lipolytica* was also not significantly different from wild-type *Y. lipolytica* (Yoga et al., 2019). These findings are in contrast to the H92R PSST mutation reported by Bajda et al. (2017), where CRISPR-Cas9 modified H92R *Drosophila* flies were not viable.

The A94V gene-edited flies did not show elevated fenpyroximate, tebufenpyrad or pyridaben resistance (Figure 3, Figure S6). Moreover, A94V mutant flies were significantly more susceptible to pyridaben compared to nos.Cas9 flies (Figure S6). In addition to toxicity tests, we also performed complex I inhibition experiments with mitochondria extracted from nos.Cas9 and A94V mutant flies. In line with the toxicity experiments, no significant differences in complex I inhibition were observed (Figure 4). This might suggest that resistance in back-crossed resistant *P. citri* lines was potentially caused by hitchhiking of a linked causal locus (an effect of linkage drag). However, as a *P. citri* genome has not yet been published, we could not investigate potential genes of importance in close proximity to the PSST gene. Alternatively, it could be that the A94V mutation has an effect only in mites and not in insects, but to investigate such hypothesis one needs to study isolated mite mitochondria directly, a procedure that proved unsuccessful in our hands for *P. citri*. The alternative, to introduce the mutation by e.g. CRISPR-Cas9, is currently also not feasible in mites.

To conclude, the rise of METI-I resistance is an important challenge in the control of herbivorous mites such as *P. citri*. PBO synergism experiments, *in vivo* enzyme assays and gene expression analysis suggest a minor involvement of P450s in fenpyroximate resistance, which is in contrast with many reported cases for *T. urticae*. Genome wide gene expression analysis also revealed distinct panels of differentially expressed genes as compared with *T. urticae*. A number

of genes were identified that might represent novel resistance genes, but need to be functionally validated. However, we identified a previously reported target-site resistance mutation, H92R in the PSST subunit of complex I, for the first time in *P. citri*, a striking demonstration of parallel molecular evolution between these species. In addition, we also identified a new mutation, A94V, in proximity of the H92R mutation and predicted to be deleterious. However, in spite of thorough investigations by marker-assisted back-crossing and mutant *Drosophila* flies, our results did not allow to make a clear claim regarding the involvement of A94V in fenpyroximate resistance.

ACKNOWLEDGEMENTS

We thank Robert Greenhalgh and Richard M. Clark for help in sequencing and analyzing mite transcriptomes, Ioannis Livadaras (IMBB-FoRTH, Crete, Greece) for injection of nos.Cas9 *Drosophila* embryos and Jan Van Arkel (University of Amsterdam, The Netherlands) for providing a photograph of an adult *P. citri* female (graphical abstract). We gratefully acknowledge financial support from Iran National Science Foundation Grant No. 96003038. This work was in part supported by the Research Foundation Flanders (FWO) [grant G009312N to TVL and grant G053815N to TVL and WD], the Research Council (ERC) under the European Union's Horizon 2020 research and innovation program [grant 772026-POLYADAPT to TVL and 773902-SuperPests to TVL and JV] and the Hellenic Foundation for Research and Innovation, HFRI (HFRI PhD Fellowship grant to RP). During this study WD was a post-doctoral fellow of the Research Foundation Flanders (FWO). SB is a post-doctoral researcher supported by ERANET, C-IPM, grant no. 618110. Illumina sequencing data for this study were generated by the Genomic Core Facility of the Health Sciences Cores at the University of Utah, USA.

Journal Pre-proof

References

Al-Hassnan, Z.N., Al-Dosary, M., Alfadhel, M., Faqeih, E.A., Alsagob, M., Kenana, R., Almass, R., Al-Harazi, O.S., Al-Hindi, H., Malibari, O.I., Almutari, F.B., Tulbah, S., Alhadeq, F., Al-Sheddi, T., Alamro, R., AlAsmari, A., Almuntashri, M., Alshaalan, H., Al-Mohanna, F.A., Colak, D., Kaya, N., 2015. ISCA2 mutation causes infantile neurodegenerative mitochondrial disorder. J. Med. Genet. 52, 186–194. https://doi.org/10.1136/jmedgenet-2014-102592

Al-Khallaf, H., 2017. Isocitrate dehydrogenases in physiology and cancer: biochemical and molecular insight. Cell Biosci. 7, 37. https://doi.org/10.1186/s13578-017-0165-3

Andrews, S., 2010. FastQC: a quality control tool for high throughput sequence data, Soil. Babraham Bioinformatics, Babraham Institute, Cambridge, United Kingdom.

Asano, S., Kamei, M., 1977. Some biological activities of cycloprate, to the citrus red mite, *Panonychus citri* (McGregor). J. Pestic. Sci. 2, 439–444. https://doi.org/10.1584/jpestics.2.439

Ay, R., Kara, F.E., 2011. Toxicity, inheritance of fenpyroximate resistance, and detoxification-enzyme levels in a laboratory-selected fenpyroximate-resistant strain of *Tetranychus urticae* Koch (Acari: Tetranychidae). Crop Prot. 30, 605–610. https://doi.org/10.1016/j.cropro.2010.11.012

Bahadorani, S., Mukai, S., Egli, D., Hilliker, A.J., 2010. Overexpression of metal-responsive transcription factor (MTF-1) in *Drosophila melanogaster* ameliorates life-span reductions associated with oxidative stress and metal toxicity. Neurobiol. Aging 31, 1215–1226. https://doi.org/10.1016/j.neurobiolaging.2008.08.001

Bajda, S., Dermauw, W., Panteleri, R., Sugimoto, N., Douris, V., Tirry, L., Osakabe, M., Vontas, J., Van Leeuwen, T., 2017. A mutation in the PSST homologue of complex I (NADH: ubiquinone oxidoreductase) from *Tetranychus urticae* is associated with resistance to METI acaricides. Insect Biochem. Mol. Biol. 80, 79–90. https://doi.org/10.1016/j.ibmb.2016.11.010

Bandyopadhyay, S., Naik, S.G., O'Carroll, I.P., Huynh, B.-H., Dean, D.R., Johnson, M.K., Dos

Santos, P.C., 2008. A proposed role for the *Azotobacter vinelandii* NfuA protein as an intermediate iron-sulfur cluster carrier. J. Biol. Chem. 283, 14092–14099. https://doi.org/10.1074/jbc.M709161200

Benjamini, Y., Hochberg, Y., 1995. Controlling the false discovery rate: a practical and powerful approach to multiple testing. J. R. Stat. Soc. Ser. B 57, 289–300. https://doi.org/10.1111/j.2517-6161.1995.tb02031.x

Bradford, M.M., 1976. A rapid and sensitive method for the quantitation of microgram quantities of protein utilizing the principle of protein-dye binding. Anal. Biochem. 72, 248–254. https://doi.org/10.1016/0003-2697(76)90527-3

Bray, N.L., Pimentel, H., Melsted, P., Pachter, L., 2016. Near-optimal probabilistic RNA-seq quantification. Nat. Biotechnol. 34, 525. https://doi.org/10.1038/nbt.3519

Budde, S.M.S., Van den Heuvel, L., Janssen, A.J., Smeets, R.J.P., Buskens, C.A.F., DeMeirleir, L., Van Coster, R., Baethmann, M., Voit, T., Trijbels, J.M.F., 2000. Combined enzymatic complex I and III deficiency associated with mutations in the nuclear encoded NDUFS4 gene. Biochem. Biophys. Res. Commun. 275, 63–68. https://doi.org/10.1006/bbrc.2000.3257

Burschel, S., Kreuzer Decovic, D., Nuber, F., Stiller, M., Hofmann, M., Zupok, A., Siemiatkowska, B., Gorka, M., Leimkühler, S., Friedrich, T., 2019. Iron-sulfur cluster carrier proteins involved in the assembly of *Escherichia coli* NADH: ubiquinone oxidoreductase (complex I). Mol. Microbiol. 111, 31–45. https://doi.org/10.1111/mmi.14137

Choi, Y., Chan, A.P., 2015. PROVEAN web server: a tool to predict the functional effect of amino acid substitutions and indels. Bioinformatics 31, 2745–2747. https://doi.org/10.1093/bioinformatics/btv195

Degli Esposti, M., 1998. Inhibitors of NADH–ubiquinone reductase: an overview. Biochim. Biophys. Acta (BBA)-Bioenergetics 1364, 222–235. https://doi.org/10.1016/S0005-2728(98)00029-2

Devine, G.J., Barber, M., Denholm, I., 2001. Incidence and inheritance of resistance to METI-

acaricides in European strains of the two-spotted spider mite (*Tetranychus urticae*)(Acari: Tetranychidae). Pest Manag. Sci. Former. Pestic. Sci. 57, 443–448. https://doi.org/10.1002/ps.307

Douris, V., Steinbach, D., Panteleri, R., Livadaras, I., Pickett, J.A., Van Leeuwen, T., Nauen, R., Vontas, J., 2016. Resistance mutation conserved between insects and mites unravels the benzoylurea insecticide mode of action on chitin biosynthesis. Proc. Natl. Acad. Sci. 113, 14692–14697. https://doi.org/10.1073/pnas.1618258113

Duarte, M., Pópulo, H., Videira, A., Friedrich, T., Schulte, U., 2001. Disruption of iron-sulphur cluster N2 from NADH: ubiquinone oxidoreductase by site-directed mutagenesis. Biochem. J. 364, 833–839. https://doi.org/10.1042/bj20011750

Finn, R.D., Attwood, T.K., Babbitt, P.C., Bateman, A., Bork, P., Bridge, A.J., Chang, H.-Y., Dosztányi, Z., El-Gebali, S., Fraser, M., 2016. InterPro in 2017—beyond protein family and domain annotations. Nucleic Acids Res. 45, D190–D199. https://doi.org/10.1093/nar/gkw1107

Friedrich, T., 1998. The NADH: ubiquinone oxidoreductase (complex I) from *Escherichia coli*. Biochim. Biophys. Acta (BBA)-Bioenergetics 1364, 134–146. https://doi.org/10.1016/s0005-2728(98)00024-3

Gotoh, T., Ishikawa, Y., Kitashima, Y., 2003. Life-history traits of the six *Panonychus* species from Japan (Acari: Tetranychidae). Exp. Appl. Acarol. 29, 241. https://doi.org/10.1023/A:1025810731386

Götz, S., García-Gómez, J.M., Terol, J., Williams, T.D., Nagaraj, S.H., Nueda, M.J., Robles, M., Talón, M., Dopazo, J., Conesa, A., 2008. High-throughput functional annotation and data mining with the Blast2GO suite. Nucleic Acids Res. 36, 3420–3435. https://doi.org/10.1093/nar/gkn176

Haas, B.J., Papanicolaou, A., Yassour, M., Grabherr, M., Blood, P.D., Bowden, J., Couger, M.B., Eccles, D., Li, B., Lieber, M., 2013. De novo transcript sequence reconstruction from RNA-seq using the Trinity platform for reference generation and analysis. Nat. Protoc. 8, 1494. https://doi.org/10.1038/nprot.2013.084

Habig, W.H., Pabst, M.J., Jakoby, W.B., 1974. Glutathione S-transferases the first enzymatic step in mercapturic acid formation. J. Biol. Chem. 249, 7130–7139.

Hall, T.A., 1999. BioEdit: a user-friendly biological sequence alignment editor and analysis program for Windows 95/98/NT, in: Nucleic Acids Symposium Series. [London]: Information Retrieval Ltd., c1979-c2000., pp. 95–98.

Hamaguchi, H., Ohshima, T., Takaishi, H., Akita, Y., Konno, T., Kajihara, O., 1990. Synthesis and acaricidal activities of fenpyroximate (NNI-850) and its related compounds, in: Abstract Papers of the 7th International Congress of Pesticide Chemistry. Springer Hamburg, Germany, pp. 5–10.

Hatefi, Y., Stiggall, D.L., 1978. [2] Preparation and properties of NADH: Cytochrome c oxidoreductase (complex I–III), in: Methods in Enzymology. Elsevier, pp. 5–10. https://doi.org/10.1016/S0076-6879(78)53005-X

Hellemans, J., Mortier, G., De Paepe, A., Speleman, F., Vandesompele, J., 2007. qBase relative quantification framework and software for management and automated analysis of real-time quantitative PCR data. Genome Biol. 8, R19. https://doi.org/10.1186/gb-2007-8-2-r19

Herron, G.A., Rophail, J., 1998. Tebufenpyrad (Pyranica®) resistance detected in two-spotted spider mite *Tetranychus urticae* Koch (Acari: Tetranychidae) from apples in Western Australia. Exp. Appl. Acarol. 22, 633–641. https://doi.org/10.1023/A:1006058705429

Hollingworth, R.M., Ahammadsahib, K.I., 1995. Inhibitors of respiratory complex I. Mechanisms, pesticidal actions and toxicology. Rev. Pestic. Toxicol. 3, 277–302.

Hollingworth, R.M., Ahammadsahib, K.I., Gadelhak, G., McLaughlin, J.L., 1994. New inhibitors of complex I of the mitochondrial electron transport chain with activity as pesticides. Biochem. Soc. Trans. 22, 230–233. https://doi.org/10.1042/bst0220230

Hospital, F., 2005. Selection in backcross programmes. Philos. Trans. R. Soc. B Biol. Sci. 360, 1503–1511. https://doi.org/10.1098/rstb.2005.1670

Jafari, I., Amiri, B., Besheli, Sharif, M.M., 2016. Comparison ability of three plant pesticides, two chemical acaricides and conventional mineral oil against citrus red mite *Panonychus citri* (McGregor) (Acarina: Tetranychidae). J. plant Prot. 30, 304–312.

https://doi.org/10.22067/jpp.v30i2.46028

Jones, V.P., Parrella, M.P., 1984. The sublethal effects of selected insecticides on life table parameters of *Panonychus citri* (Acari: Tetranychidae). Can. Entomol. 116, 1033–1040. https://doi.org/10.4039/Ent1161033-7

Jum, B.C., Young, J.K., Young, J.A., Jai, K.Y., Jeong, O.L., 1995. Monitoring of acaricide resistance in field-collected populations of *Tetranychus urticae* (Acari: Tetranychidae) in Korea. Korean J. Appl. Entomol. 34, 40–45.

Khalighi, M., Dermauw, W., Wybouw, N., Bajda, S., Osakabe, M., Tirry, L., Van Leeuwen, T., 2016. Molecular analysis of cyenopyrafen resistance in the two spotted spider mite *Tetranychus urticae*. Pest Manag. Sci. 72, 103–112. https://doi.org/10.1002/ps.4071

Kim, Y., Lee, Si-Hyeock, Lee, Si-Woo, Ahn, Y., 2004. Fenpyroximate resistance in *Tetranychus urticae* (Acari: Tetranychidae): cross-resistance and biochemical resistance mechanisms. Pest Manag. Sci. Former. Pestic. Sci. 60, 1001–1006. https://doi.org/10.1002/ps.909

Konno, T., Kuriyama, K., Hamaguchi, H., 1990. Fenpyroximate (NNI-850), a new acaricide, in: Brighton Crop Protection Conference. Pests and Diseases-1990. Vol. 1. British Crop Protection Council, pp. 71–78.

Korge, P., Calmettes, G., Weiss, J.N., 2016. Reactive oxygen species production in cardiac mitochondria after complex I inhibition: Modulation by substrate-dependent regulation of the NADH/NAD+ ratio. Free Radic. Biol. Med. 96, 22–33. https://doi.org/10.1016/j.freeradbiomed.2016.04.002

Kumral, N.A., Kovanci, B., 2007. Susceptibility of female populations of *Panonychus ulmi* (Koch)(Acari: Tetranychidae) to some acaricides in apple orchards. J. Pest Sci. (2004). 80, 131–137. https://doi.org/10.1007/s10340-007-0163-z

Larosa, V., Remacle, C., 2018. Insights into the respiratory chain and oxidative stress. Biosci. Rep. 38, BSR20171492. https://doi.org/10.1042/BSR20171492

Li, W., Godzik, A., 2006. Cd-hit: a fast program for clustering and comparing large sets of protein or nucleotide sequences. Bioinformatics 22, 1658–1659. https://doi.org/10.1093/bioinformatics/btl158

Lümmen, P., 1998. Complex I inhibitors as insecticides and acaricides. Biochim. Biophys. Acta (BBA)-Bioenergetics 1364, 287–296. https://doi.org/10.1016/S0005-2728(98)00034-6

Magnitsky, S., Toulokhonova, L., Yano, T., Sled, V.D., Hägerhäll, C., Grivennikova, V.G., Burbaev, D.S., Vinogradov, A.D., Ohnishi, T., 2002. EPR characterization of ubisemiquinones and iron–sulfur cluster N2, central components of the energy coupling in the NADH-ubiquinone oxidoreductase (complex I) in situ. J. Bioenerg. Biomembr. 34, 193–208. https://doi.org/10.1023/A:1016083419979

Melber, A., Na, U., Vashisht, A., Weiler, B.D., Lill, R., Wohlschlegel, J.A., Winge, D.R., 2016. Role of Nfu1 and Bol3 in iron-sulfur cluster transfer to mitochondrial clients. Elife 5, e15991. https://doi.org/10.7554/eLife.15991

Mota-Sanchez, D., Wise., J.C., 2019. The Arthropod Pesticide Resistance Database. Michigan State Univ. URL http://www.pesticideresistance.org

Nauen, R., Stumpf, N., Elbert, A., Zebitz, C.P.W., Kraus, W., 2001. Acaricide toxicity and resistance in larvae of different strains of *Tetranychus urticae* and *Panonychus ulmi* (Acari: Tetranychidae). Pest Manag. Sci. Former. Pestic. Sci. 57, 253–261. https://doi.org/doi.org/10.1002/ps.220

Naveira, H., Barbadilla, A., 1992. The theoretical distribution of lengths of intact chromosome segments around a locus held heterozygous with backcrossing in a diploid species. Genetics 130, 205–209.

Niu, J.-Z., Dou, W., Ding, T.-B., Yang, L.-H., Shen, G.-M., Wang, J.-J., 2012. Evaluation of suitable reference genes for quantitative RT-PCR during development and abiotic stress in *Panonychus citri* (McGregor)(Acari: Tetranychidae). Mol. Biol. Rep. 39, 5841–5849. https://doi.org/10.1007/s11033-011-1394-x

Nourbakhsh, S., 2018. List of important pests, diseases and weeds of major agricultural crops, pesticides and recommended methods for their control. Ministry of Jihad-e- Agriculture, Plant Protection Organization, Iran.

Ozawa, A., 1994. Acaricides susceptibility of Kanzawa spider mite, *Tetranychus kanzawai* Kishida (Acarina; Tetranychidae) collected from tea fields in Chuuen and Ogasa district in

Shizuoka prefecture. Chagyo Kenkyu Hokoku (Tea Res. Journal) 1994, 1–14. https://doi.org/10.5979/cha.1994.1

Pan, W., Luo, P., Fu, R., Gao, P., Long, Z., Xu, F., Xiao, H., Liu, S., 2006. Acaricidal activity against *Panonychus citri* of a ginkgolic acid from the external seed coat of *Ginkgo biloba*. Pest Manag. Sci. Former. Pestic. Sci. 62, 283–287. https://doi.org/10.1002/ps.1152

Petruzzella, V., Vergari, R., Puzziferri, I., Boffoli, D., Lamantea, E., Zeviani, M., Papa, S., 2001. A nonsense mutation in the NDUFS4 gene encoding the 18 kDa (AQDQ) subunit of complex I abolishes assembly and activity of the complex in a patient with Leigh-like syndrome. Hum. Mol. Genet. 10, 529–536. https://doi.org/10.1093/hmg/10.5.529

Pimentel, H., Bray, N.L., Puente, S., Melsted, P., Pachter, L., 2017. Differential analysis of RNA-seq incorporating quantification uncertainty. Nat. Methods 14, 687. https://doi.org/10.1038/nmeth.4324

Porpaczy, Z., Sumegi, B., Alkonyi, I., 1987. Interaction between NAD-dependent isocitrate dehydrogenase, alpha-ketoglutarate dehydrogenase complex, and NADH: ubiquinone oxidoreductase. J. Biol. Chem. 262, 9509–9514.

Ran, C., Chen, Y., Wang, J.-J., 2009. Susceptibility and carboxylesterase activity of five field populations of *Panonychus citri* (McGregor)(Acari: Tetranychidae) to four acaricides. Int. J. Acarol. 35, 115–121. https://doi.org/10.1080/01647950902917593

Riga, M., Myridakis, A., Tsakireli, D., Morou, E., Stephanou, E.G., Nauen, R., Van Leeuwen, T., Douris, V., Vontas, J., 2015. Functional characterization of the *Tetranychus urticae* CYP392A11, a cytochrome P450 that hydroxylates the METI acaricides cyenopyrafen and fenpyroximate. Insect Biochem. Mol. Biol. 65, 91–99. https://doi.org/10.1016/j.ibmb.2015.09.004

Ritz, C., Baty, F., Streibig, J.C., Gerhard, D., 2015. Dose-response analysis using R. PLoS One 10, e0146021. https://doi.org/10.1371/journal.pone.0146021

Robertson, J.L., Jones, M.M., Olguin, E., Alberts, B., 2017. Bioassays with arthropods. CRC press. https://doi.org/10.1201/9781315373775

Rodenhouse, N.L., Best, L.B., O'Connor, R.J., Bollinger, E.K., 2004. SAS Institute Inc, in: SAS.

p. 3.

Rozen, S., Skaletsky, H., 2000. Primer3 on the WWW for general users and for biologist programmers, in: Bioinformatics Methods and Protocols. Springer, pp. 365–386. https://doi.org/10.1385/1-59259-192-2:365

Sahraeian, S.M.E., Mohiyuddin, M., Sebra, R., Tilgner, H., Afshar, P.T., Au, K.F., Asadi, N.B., Gerstein, M.B., Wong, W.H., Snyder, M.P., 2017. Gaining comprehensive biological insight into the transcriptome by performing a broad-spectrum RNA-seq analysis. Nat. Commun. 8, 59. https://doi.org/10.1038/s41467-017-00050-4

Saini, N., Georgiev, O., Schaffner, W., 2011. The parkin mutant phenotype in the fly is largely rescued by metal-responsive transcription factor (MTF-1). Mol. Cell. Biol. 31, 2151–2161. https://doi.org/10.1128/MCB.05207-11

Samantsidis, G.-R., O'Reilly, A.O., Douris, V., Vontas, J., 2019. Functional validation of target-site resistance mutations against sodium channel blocker insecticides (SCBIs) via molecular modeling and genome engineering in *Drosophila*. Insect Biochem. Mol. Biol. 104, 73–81. https://doi.org/10.1016/j.ibmb.2018.12.006

Schuler, F., Yano, T., Di Bernardo, S., Yagi, T., Yankovskaya, V., Singer, T.P., Casida, J.E., 1999. NADH-quinone oxidoreductase: PSST subunit couples electron transfer from iron–sulfur cluster N2 to quinone. Proc. Natl. Acad. Sci. 96, 4149–4153. https://doi.org/10.1073/pnas.96.7.4149

Sheftel, A.D., Wilbrecht, C., Stehling, O., Niggemeyer, B., Elsässer, H.-P., Mühlenhoff, U., Lill, R., 2012. The human mitochondrial ISCA1, ISCA2, and IBA57 proteins are required for [4Fe-4S] protein maturation. Mol. Biol. Cell 23, 1157–1166. https://doi.org/10.1091/mbc.e11-09-0772

Sherer, T.B., Richardson, J.R., Testa, C.M., Seo, B.B., Panov, A. V, Yagi, T., Matsuno-Yagi, A., Miller, G.W., Greenamyre, J.T., 2007. Mechanism of toxicity of pesticides acting at complex I: relevance to environmental etiologies of Parkinson's disease. J. Neurochem. 100, 1469–1479. https://doi.org/10.1111/j.1471-4159.2006.04333.x

Shiraishi, Y., Murai, M., Sakiyama, N., Ifuku, K., Miyoshi, H., 2012. Fenpyroximate binds to the

interface between PSST and 49 kDa subunits in mitochondrial NADH-ubiquinone oxidoreductase. Biochemistry 51, 1953–1963. https://doi.org/10.1021/bi300047h

Shiryev, S.A., Papadopoulos, J.S., Schäffer, A.A., Agarwala, R., 2007. Improved BLAST searches using longer words for protein seeding. Bioinformatics 23, 2949–2951. https://doi.org/10.1093/bioinformatics/btm479

Snoeck, S., Kurlovs, A.H., Bajda, S., Feyereisen, R., Greenhalgh, R., Villacis-Perez, E., Kosterlitz, O., Dermauw, W., Clark, R.M., Van Leeuwen, T., 2019. High-resolution QTL mapping in *Tetranychus urticae* reveals acaricide-specific responses and common target-site resistance after selection by different METI-I acaricides. Insect Biochem. Mol. Biol. 110, 19–33. https://doi.org/10.1016/j.ibmb.2019.04.011

Stumpf, N., Nauen, R., 2001. Cross-resistance, inheritance, and biochemistry of mitochondrial electron transport inhibitor-acaricide resistance in *Tetranychus urticae* (Acari: Tetranychidae). J. Econ. Entomol. 94, 1577–1583. https://doi.org/10.1603/0022-0493-94.6.1577

Sugimoto, N., Osakabe, M., 2014. Cross-resistance between cyenopyrafen and pyridaben in the two spotted spider mite *Tetranychus urticae* (Acari: Tetranychidae). Pest Manag. Sci. 70, 1090–1096. https://doi.org/10.1002/ps.3652

Tsagkarakou, A., Van Leeuwen, T., Khajehali, J., Ilias, A., Grispou, M., Williamson, M.S., Tirry, L., Vontas, J., 2009. Identification of pyrethroid resistance associated mutations in the para sodium channel of the two-spotted spider mite *Tetranychus urticae* (Acari: Tetranychidae). Insect Mol. Biol. 18, 583–593. https://doi.org/10.1111/j.1365-2583.2009.00900.x

Van Asperen, K., 1962. A study of housefly esterases by means of a sensitive colorimetric method. J. Insect Physiol. 8, 401–416. https://doi.org/10.1016/0022-1910(62)90074-4

Van Leeuwen, T., Tirry, L., Yamamoto, A., Nauen, R., Dermauw, W., 2015. The economic importance of acaricides in the control of phytophagous mites and an update on recent acaricide mode of action research. Pestic. Biochem. Physiol. 121, 12–21. https://doi.org/10.1016/j.pestbp.2014.12.009

Van Leeuwen, T., Van Pottelberge, S., Tirry, L., 2005. Comparative acaricide susceptibility and detoxifying enzyme activities in field-collected resistant and susceptible strains of *Tetranychus urticae*. Pest Manag. Sci. Former. Pestic. Sci. 61, 499–507. https://doi.org/10.1002/ps.1001

Van Leeuwen, T., Vontas, J., Tsagkarakou, A., Tirry, L., 2009. Mechanisms of acaricide resistance in the two-spotted spider mite *Tetranychus urticae*, in: Biorational Control of Arthropod Pests. Springer, pp. 347–393. https://doi.org/10.1007/978-90-481-2316-2_14

Van Pottelberge, S., Van Leeuwen, T., Nauen, R., Tirry, L., 2009. Resistance mechanisms to mitochondrial electron transport inhibitors in a field-collected strain of *Tetranychus urticae* Koch (Acari: Tetranychidae). Bull. Entomol. Res. 99, 23–31. https://doi.org/10.1017/S0007485308006081

Vassiliou, V.A., Papadoulis, G., 2009. First record of the citrus red mite *Panonychus citri* in Cyprus. Phytoparasitica 37, 99–100. https://doi.org/10.1007/s12600-008-0017-0

Wirth, C., Brandt, U., Hunte, C., Zickermann, V., 2016. Structure and function of mitochondrial complex I. Biochim. Biophys. Acta (BBA)-Bioenergetics 1857, 902–914. https://doi.org/10.1016/j.bbabio.2016.02.013

Wood Jr, F.E., Nordin, J.H., 1980. Temperature effects on mitochondrial respiration of *Protophormia terranovae* and *Musca domestica*. Insect Biochem. 10, 95–99. https://doi.org/10.1016/0020-1790(80)90044-X

Yamamoto, A., Yoneda, H., Hatano, R., Asada, M., 1995. Laboratory selections of populations in the citrus red mite, *Panonychus citri* (McGregor), with hexythiazox and their cross resistance spectrum. J. Pestic. Sci. 20, 493–501. https://doi.org/10.1584/jpestics.20.493

Yoga, E.G., Haapanen, O., Wittig, I., Siegmund, K., Sharma, V., Zickermann, V., 2019. Mutations in a conserved loop in the PSST subunit of respiratory complex I affect ubiquinone binding and dynamics. Biochim. Biophys. Acta. https://doi.org/10.1016/j.bbabio.2019.06.006

Young, M.D., Wakefield, M.J., Smyth, G.K., Oshlack, A., 2010. Gene ontology analysis for RNA-seq: accounting for selection bias. Genome Biol. 11, R14. https://doi.org/10.1186/gb-

2010-11-2-r14

Zimbler, D.L., Park, T.M., Arivett, B.A., Penwell, W.F., Greer, S.M., Woodruff, T.M., Tierney, D.L., Actis, L.A., 2012. Stress response and virulence functions of the *Acinetobacter baumannii* NfuA Fe-S scaffold protein. J. Bacteriol. 194, 2884–2893. https://doi.org/10.1128/JB.00213-12

Journal Pre-proof

Figure Legends

Figure 1 - Transcriptome analysis of three fenpyroximate resistant *P. citri* populations. (A) Volcano plot depicting differentially expressed transcripts between the fenpyroximate resistant strains (Sari, Ramsar and Lahijan) and the fenpyroximate susceptible strain Rasht. Differentially expressed transcripts with an absolute $log_2FC \geq 1$ are coloured in red. (B) PCA plot of gene expression levels of all four *P. citri* populations. For each population, Rasht, Lahijan, Ramsar and Sari, convex hulls were added for easier visual interpretation. (C) Venn diagram depicting overlap among differentially expressed transcripts (red: overexpressed, blue: underexpressed) in adult *P. citri* females from the three fenpyroximate resistant populations (Sari, Ramsar and Lahijan) compared to adults from the susceptible Rasht population ($log_2FC \geq 1$, q-value ≤ 0.05).

Figure 2 - Frequency of H92R and A94V mutations in single males of four populations of *P.citri*. A) Alignment of a *P. citri* PSST fragment with those of other Metazoa, *Yarrowia lipolytica* and *T. aquaticus*. The H92R and A94V mutation (*Y. lipolytica* numbering) are indicated with an asterisk. *B. taurus* PSST residues that were photoaffinity labeled by a photoreactive derivative of fenpyroximate are indicated in grey font (Shiraishi et al., 2012). B) Bar plot showing A94V and H92R frequency in 20 males of Rasht (susceptible population), Lahijan, Ramsar and Sari (resistant populations).

Figure 3 - Toxicity of fenpyroximate to A94V mutant and nos.Cas9 fly lines as assessed by a topical assay. No significant differences (as assessed by a Mann-Whitney-U test) in mean fenpyroximate mortality were found between the different lines.

Figure 4 - Dose-response relationships of tebufenpyrad, fenpyroximate and pyridaben to the inhibition of complex I of nos.Cas9 and A94V fly lines. METI-I inhibition is expressed as % inhibition compared to inhibition by 100 nM fenazaquin.

Journal Pre-proof

Tables

Table 1 - Toxicity of fenpyroximate with and without synergists to female adults of *P. citri*

Population	Treatment	n[a]	LC_{50} (mg a.i. L^{-1})[b]	Slope±SE	X^2(df)	RR(95% CI)[c]	SR(95% CI)[d]
Rasht	fenpyroximate	240	6.572 (5.850-7.464)	4.309± 0.674	0.492(2)		
	PBO	240	2.261 (1.803-3.028)*	2.249± 0.368	0.608 (2)		2.953 (2.244-3.885)
	DEM	240	6.540 (5.840-7.382)	4.436 ±0.706	1.818 (2)		1.034 (0.882-1.213)
	TPP	240	5.263 (4.156-7.406)	2.100 ± 0.398	0.263 (2)		1.285 (0.960-1.720)
Gorgan	fenpyroximate	240	47.690 (27.273-84.616)	2.056 ±0.352	4.624 (3)	7.257 (5.699-9.240)	
	PBO	240	14.777 (9.625-22.243)*	3.696 ±0.434	7.533 (3)	6.537(4.930-8.668)	3.227 (2.514-4.143)
	DEM	240	39.068 (32.544-52.575)	2.650±0.581	1.052 (2)	5.695 (4.716- 6.879)	1.221 (0.904-1.649)
	TPP	240	24.661 (19.158-35.073)*	1.916± 0.384	0.676 (2)	4.129(2.965-5.750)	1.934 (1.362- 2.745)
Rahimabad	fenpyroximate	240	46.193 (38.111-57.284)	2.270±0.351	2.939 (3)	7.029 (5.582-8.851)	
	PBO	240	7.318 (6.236-8.991)*	3.079± 0.552	1.208 (2)	3.036 (2.295-4.017)	6.313 (4.852-8.212)
	DEM	240	31.048 (26.628-36.761)*	3.209±0.588	0.113 (2)	4.729 (3.946-5.668)	1.737(1.355-2.228)
	TPP	240	18.117 (14.759-23.871)*	2.456± 0.419	0.366 (2)	3.337 (2.412-4.617)	2.978 (2.204-4.023)
Talesh	fenpyroximate	240	130.389 (105.711-166.619)	2.048±0.358	2.234 (3)	19.840 (15.49-25.412)	
	PBO	240	25.299 (21.055-31.462)*	2.680± 0.44	1.499 (2)	10.822 (8.041-14.565)	5.154 (3.853-6.894)
	DEM	240	94.989 (77.552-117.239)*	2.487±0.436	2.145 (2)	13.747 (11.258-16.787)	1.373 (1.023-1.842)
	TPP	240	65.086 (56.197-75.777)*	3.452± 0.56	1.184 (2)	12.521(9.228-16.990)	2.003 (1.543-2.601)
Lahijan	fenpyroximate	240	131.980 (118.429-147.434)	4.160 ± 0.862	1.365 (3)	19.883 (15.979-24.740)	
	PBO	240	31.153 (23.814-43.954)*	1.778± 0.42	0.240 (2)	12.623 (9.162-17.391)	4.237 (3.154-5.691)
	DEM	240	113.636 (97.982-143.770)	3.384± 0.631	0.275 (2)	16.442 (13.959-19.367)	1.161 (0.946-1.426)
	TPP	240	97.295 (82.270-125.775)*	3.183 ± 0.571	0.525 (2)	17.794 (12.743-24.846)	1.356 (1.083-1.699)
Ramsar	fenpyroximate	240	> 500			> 76.08	
	PBO	240	> 500			> 221.141	/
	DEM	240	> 500			> 76.542	/
	TPP	240	> 500			> 95.002	/
Sari	fenpyroximate	240	> 500			> 76.08	
	PBO	240	> 500			> 221.141	/
	DEM	240	> 500			> 76.542	/
	TPP	240	> 500			> 95.002	/

[a] the total number of mites used for all concentrations

[b] the LC50 value is expressed as mg a.i. L^{-1} and their 95% confidence intervals (95% CI); an asterisk indicates whether there is a significant difference between synergist+fenpyroximate treatment and treatment with fenpyroximate alone (based on 95% CI of SR)

[c]RR, Resistance ratio= LC_{50} of acaricide/LC_{50} of susceptible (Rasht) population

[d]SR, Synergistic ratio= LC_{50} of acaricide/LC_{50} of (synergist + acaricide);

Journal Pre-proof

Table 2 - Toxicity of pyridaben and tebufenpyrad to four populations of *P. citri*

Treatment	Population	n[a]	LC_{50} (mg a.i. L^{-1})[b]	Slope ± SE	X^2(df)	RR(95% CI)[c]
pyridaben	Rasht	240	0.918 (0.596-1.446)	1.518±0.979	0.861 (3)	
	Lahijan	240	2.510 (1.408-4.043)	1.632±0.150	5.813 (3)	2.733 (1.280-5.150)
	Ramsar	240	4.178 (3.195-5.493)	1.751±0.150	3.957 (3)	4.703 (3.210-6.810)
	Sari	240	28.740 (25.450-32.250)	2.178±0.210	1.752 (3)	31.725 (26.780-37.301)
tebufenpyrad	Rasht	240	4.104 (3.520-4.760)	0.461±0.069	0.991 (3)	
	Lahijan	240	77.844 (68.850-88.690)	3.407±0.306	4.392 (3)	18.967 (15.660-23.201)
	Ramsar	240	83.965 (63.920-109.490)	6.595±0.577	2.607 (3)	23.490 (15.580-34.710)
	Sari	240	937.770 (844.810-1041.780)	2.890±0.271	2.487 (3)	259.250 (223.670-300.240)

[a] the total number of mites used for all concentrations
[b] the LC_{50} value is expressed as mg a.i. L^{-1} and their 95% confidence intervals (95% CI)
[c] RR, Resistance ratio= LC_{50} of acaricide/LC_{50} of susceptible (Rasht) population

Journal Pre-proof

Table 3 - Detoxification enzyme activities in different populations of *P. citri* (mean ± SEM).

Population	α-NA (µmol/min/mg protein) ±SE	Ratio	β-NA (µmol/min/mg protein) ±SE	Ratio	CDNB (µmol/min/mg protein) ±SE	Ratio	7-EFC (pmol/mg protein/30 min) ± SE	Ratio
Rasht	0.328±0.024^{c*}		0.205±0.037^{bc}		0.249±0.025^{b}		1529.758±35.61^{b}	
Gorgan	2.019±0.035^{a}	6.155	0.733±0.053^{a}	3.575	0.547±0.028^{a}	2.196	n.d.	
Rahimabad	0.211±0.024^{c}	0.643	0.122±0.018^{c}	0.595	0.303±0.011^{b}	1.216	n.d.	
Talesh	0.760±0.225^{b}	2.317	0.324±0.043^{b}	1.580	0.546±0.014^{a}	2.192	n.d.	
Lahijan	0.271±0.011^{c}	0.826	0.092±0.013^{c}	0.448	0.240±0.012^{b}	0.963	2493.141±354.43^{a}	1.629
Ramsar	0.116±0.034^{d}	0.353	0.021±0.002^{c}	0.102	0.302±0.035^{b}	1.212	1482.335±174.63^{b}	0.968
Sari	0.178±0.022^{cd}	0.542	0.065±0.004^{c}	0.317	0.196±0.020^{b}	0.787	1898.310±171.37^{ab}	1.240

*means followed by the same letter in a column are not significantly different at 5% probability level (Tukey).
n.d.: not determined

Journal Pre-proof

Table 4 - Toxicity of fenpyroximate and pyridaben to female adults of *P. citri* of back-crossed lines S1 and S2 (A94/A94 genotype), back-crossed lines R1 and R2 (V94/V94 genotype) and their parental strains (Rasht and Lahijan populations)

Treatment	Strain /Line	n[a]	LC_{50} (mg a.i. L^{-1})[b]	Slope (± SE)	X^2 (df)	RR (95% CI)[c]
fenpyroximate	Rasht	240	6.572 (5.544-7.983)	4.309 ± 0.953	0.492 (2)	
	S1	240	4.677(3.673-5.893)	2.221 ± 0.356	0.754 (5)	0.712 (0.536-0.945)
	R1	240	60.259(36.669-116.820)	1.112 ± 0.225	3.462 (4)	9.169 (5.224-16.094)
	S2	240	5.361 (3.887-8.270)	1.644 ± 0.364	3.445 (4)	0.816 (0.701-1.035)
	R2	240	70.167 (45.643-135.906)	4.309 ± 0.953	2.374 (8)	10.677 (6.242-18.261)
	Lahijan	240	131.980(112.492-155.660)	4.160 ± 0.[illegible]62	0.365 (3)	19.883 (15.979-24.740)
pyridaben	Rasht	240	0.918 (0.596-1.446)	1.5[illegible]3±0.979	0.861 (3)	
	S1	240	0.587 (0.456-0.807)	2.60[illegible] ± 0.565	1.905 (3)	0.637 (0.480-0.844)
	R1	240	1.665 (1.337-2.073)	2.82[illegible] ± 0.489	0.152 (4)	1.736 (1.352-2.229)
	S2	240	0.756 (0.436-2.[illegible]0)	1.468 ± 0.443	1.643 (2)	0.823 (0.731-1.728)
	R2	240	1.365 (0.[illegible]77-1.[illegible]06)	2.349 ± 0.482	0.029 (2)	1.423 (1.013-1.999)
	Lahijan	240	2.510 (1.[illegible]98-4.043)	1.632 ± 0.15	5.813 (3)	2.733 (1.280-5.150)

[a] the total number of mites used for all concentrations
[b] the LC_{50} value is expressed as mg a.i. L^{-1} and their 95% confidence intervals (95% CI)
[c] RR, Resistance ratio= LC_{50} of acaricide/LC_{50} of susceptible (Rasht) population

Journal Pre-proof

Supplementary Information

Supplementary Figures

Figure S1 - Map of collection sites of *P. citri* populations from citrus growing regions of Northern provinces of Iran

Figure S2 - CRISPR/Cas9 strategy for generation of genome modified flies bearing PSST A94V mutation.
Nucleotide and deduced amino acid sequence of a 873 bp fragment of *CG9172 (ND20)*, encompassing the *Drosophila melanogaster* amino acid sequence. Light gray areas indicate the CRISPR/Cas9 targets selected (sgRNA1, sgRNA2, see also Bajda *et al.*, 2017), while dark gray areas indicate the corresponding PAM (-*NGG*) triplets. Vertical arrows denote break points for CRISPR/Cas9-induced double stranded breaks. An oval circle marks the non-synonymous difference (A94V, *Y. lipolytica* numbering, corresponding to *Drosophila* PSST A105V) between target (wild-type) and donor (genome modified) sequences. Synonymous mutations incorporated for diagnostic purposes, as well as to avoid cleavage of the donor plasmid by the CRISPR/Cas9 machinery, are shown above the nucleotide sequence. Restriction site Tsp45I, abolished due to genome modification, is shown with strikethrough letters and the corresponding sequence is underlined. Restriction site SgrBI, introduced because of the genome modification, is shown in a dashed box and the corresponding sequence is also underlined. Horizontal arrows indicate the positions of primer pair CG9172_ver F/R (Table S4) used for sequencing of the genome modified alleles.

Figure S3 - Screening for genome-modified flies.
A) PCR screening of individual G_1 flies derived from different G_0 (injected) individuals using a specific primer pair (CG9172_dia F/R) that generates a 294 bp diagnostic fragment for A94V (*Y. lipolytica* numbering, corresponding to *Drosophila* A105V) mutation positives [-: nos.Cas9 DNA (negative control), +: donor plasmid template (positive control)]. B) Screening of G_1 flies for A94V allele following PCR amplification with a "generic" primer pair (CG9172_ver F/R), and digestion of the 559 bp product with SgrBI. The wild-type allele remains uncut, while the genome modified A94V allele is cut in two smaller bands of 328 and 231 bp respectively [-: nos.Cas9 DNA (negative control), +: donor plasmid template (positive control)]. C) Sequencing of the relevant PSST (ND20) region in homozygous genome modified flies. The deduced amino acid sequence is shown on top of the nucleotide sequence. Ovals indicate nucleotides differing in relation to the wild-type sequence. The genome modified GTT codon (A94V) is shown within a dashed square. The SgrBI site introduced is underlined.

Figure S4 - *Drosophila* crossing scheme for genome modification in the X chromosome (modified from Samantsidis et al., 2019). Several nos.Cas9 G_0 embryos were injected and surviving adults back-crossed to nos.Cas9. The G_1 progeny is sampled (n≈30) and screened as described in section 2.10.2. Individual G_1 flies from positive original G_0 crosses were back-crossed with nos.Cas9 and after generating G_2 progeny, they underwent molecular screening (single fly PCR) for homologous directed repair (HDR). Positive crosses now contain the mutant allele in 50% of the G_2 progeny. Individual female G_2 flies were then crossed with male flies carrying a balancer X chromosome (FM7c *Hw w B*) with a characteristic phenotypic marker

(*Bar*) and after producing G_3 progeny, they were again individually screened to identify positive crosses. Individual G_3 females with heterozygous *Bar* phenotype are crossed to the balancer strain males and then screened for HDR. G_4 females with *Bar* phenotype (bearing the desired mutation opposite to FM7c) are crossed with male siblings selected against *Bar* (i.e. hemizygous for the genome modified chromosome bearing the HDR-derived allele) and their progeny (G_5) is selected against *Bar* to generate homozygous lines bearing the desired mutations.

Figure S5 - RT-qPCR validation of a selection of DETs between the Sari and Rasht population. Error bars represent 95% CI, while an asterisk indicates significant (p-value < 0.05) expression differences between Sari and Rasht.

Figure S6 - Toxicity of tebufenpyrad, pyridaben and fenpyroximate to A94V mutant and nos.Cas9 fly lines as assessed by contact assays. Significant differences in mean mortality, as assessed by a Mann-Whitney-U test are indicated with an asterisk.

Supplementary Files

File S1 - Sequence of PSST in donor plasmid (FASTA format)

File S2 - Merged *P. citri* transcriptome assembly (FASTA-format).

File S3 - Transcriptome assembly of the Rasht, Lahijan, Ramsar and Sari *P. citri* population.

Supplementary Tables

Table S1 - Kallisto read mapping statistics against the merged transcriptome *P. citri* assembly (File S2)

Table S2 - Blast2GO analysis of the merged transcriptome assembly (File S2).

Table S3 - *Citrus* sp. or viral transcripts that were removed before differential transcript expression analysis

Table S4 - Primers used in this study

Table S5 - Conditions and components for PCR experiments with *P. citri* DNA

Table S6 - Differentially expressed transcripts between the fenpyroximate resistant *P. citri* populations Lahijan, Ramsar and Sari and the susceptible populations Rasht.

Table S7 - Overlap between differentially expressed transcripts of the fenpyroximate resistant *P. citri* populations

Table S8 - Significantly enriched GO-terms in differentially expressed transcripts between the moderately fenpyroximate resistant Lahijan population and the susceptible Rasht population

Journal Pre-proof

- fenpyroximate resistance was investigated in seven *Panonychus citri* populations from Iran
- fenpyroximate resistance ratios reached up to 75-fold and cross-resistance with other METI-I acaricides was observed
- PBO synergism experiments, *in vivo* assays and expression analysis suggest a minor role for P450s in fenpyroximate resistance
- a H92R mutation in the PSST subunit, previously associated with METI-I target-site resistance, was detected in a highly resistant *P. citri* population
- a new PSST mutation, A94V, was detected in a resistant population but no clear claim regarding its role in resistance could be made

Journal Pre-proof

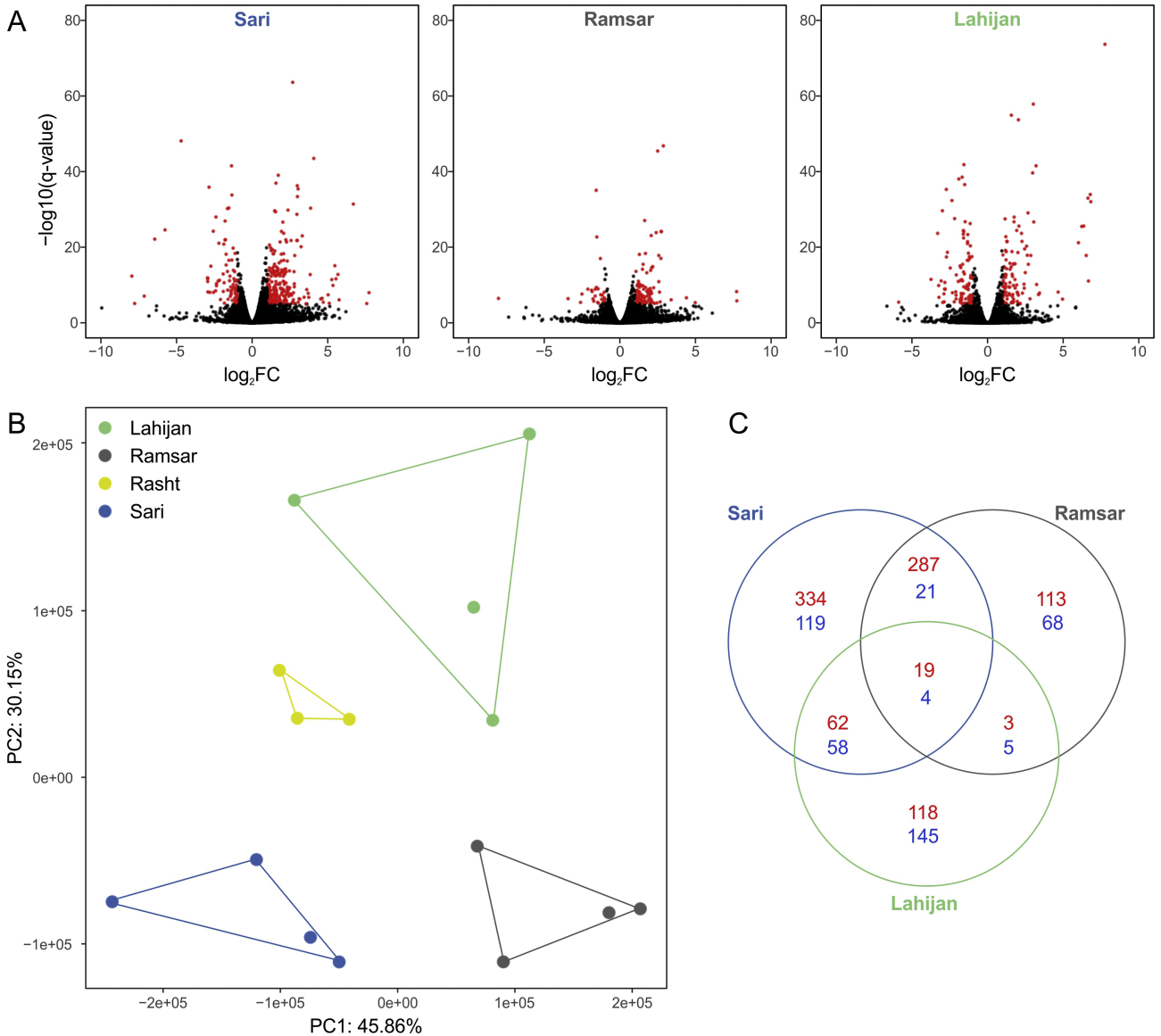
A
Sari
Ramsar
Lahijan
−log10(q-value)
log2FC
B
Lahijan
Ramsar
Rasht
Sari
PC2: 30.15%
PC1: 45.86%
C
Sari
Ramsar
Lahijan
334
119
287
21
113
68
19
4
62
58
3
5
118
145

Figure 1

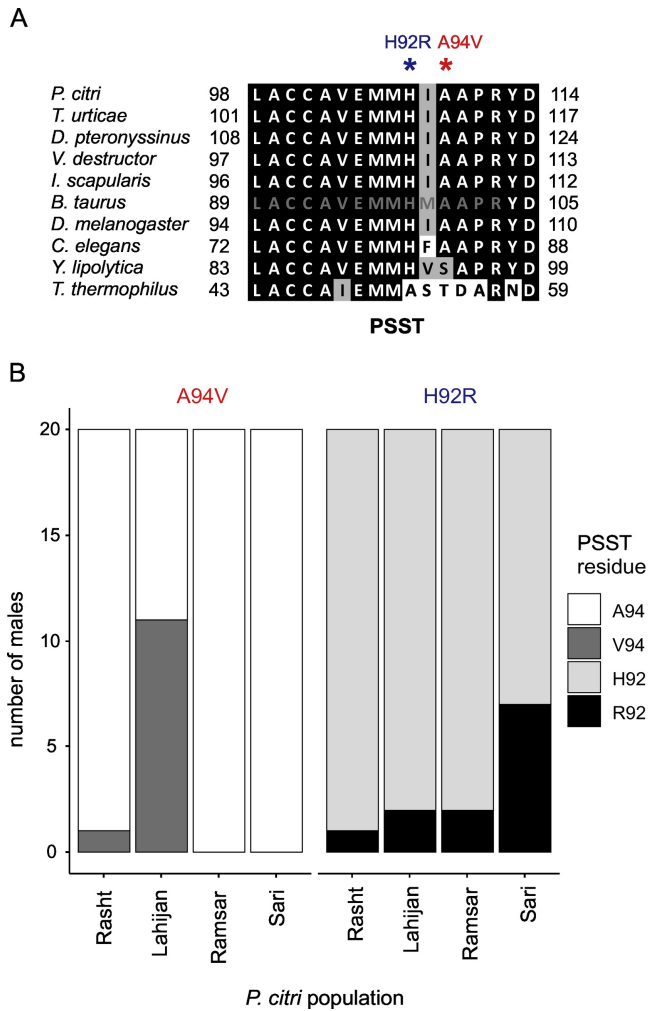
A
H92R A94V
P. citri 98 LACCAVEMMHIAAPRYD 114
T. urticae 101 LACCAVEMMHIAAPRYD 117
D. pteronyssinus 108 LACCAVEMMHIAAPRYD 124
V. destructor 97 LACCAVEMMHIAAPRYD 113
I. scapularis 96 LACCAVEMMHIAAPRYD 112
B. taurus 89 LACCAVEMMHMAAPRYD 105
D. melanogaster 94 LACCAVEMMHIAAPRYD 110
C. elegans 72 LACCAVEMMHFAAPRYD 88
Y. lipolytica 83 LACCAVEMMHVSAPRYD 99
T. thermophilus 43 LACCAIEMMASTDARND 59
PSST
B
A94V
H92R
number of males
20
15
10
5
0
PSST residue
A94
V94
H92
R92
Rasht
Lahijan
Ramsar
Sari
Rasht
Lahijan
Ramsar
Sari
P. citri population

Figure 2

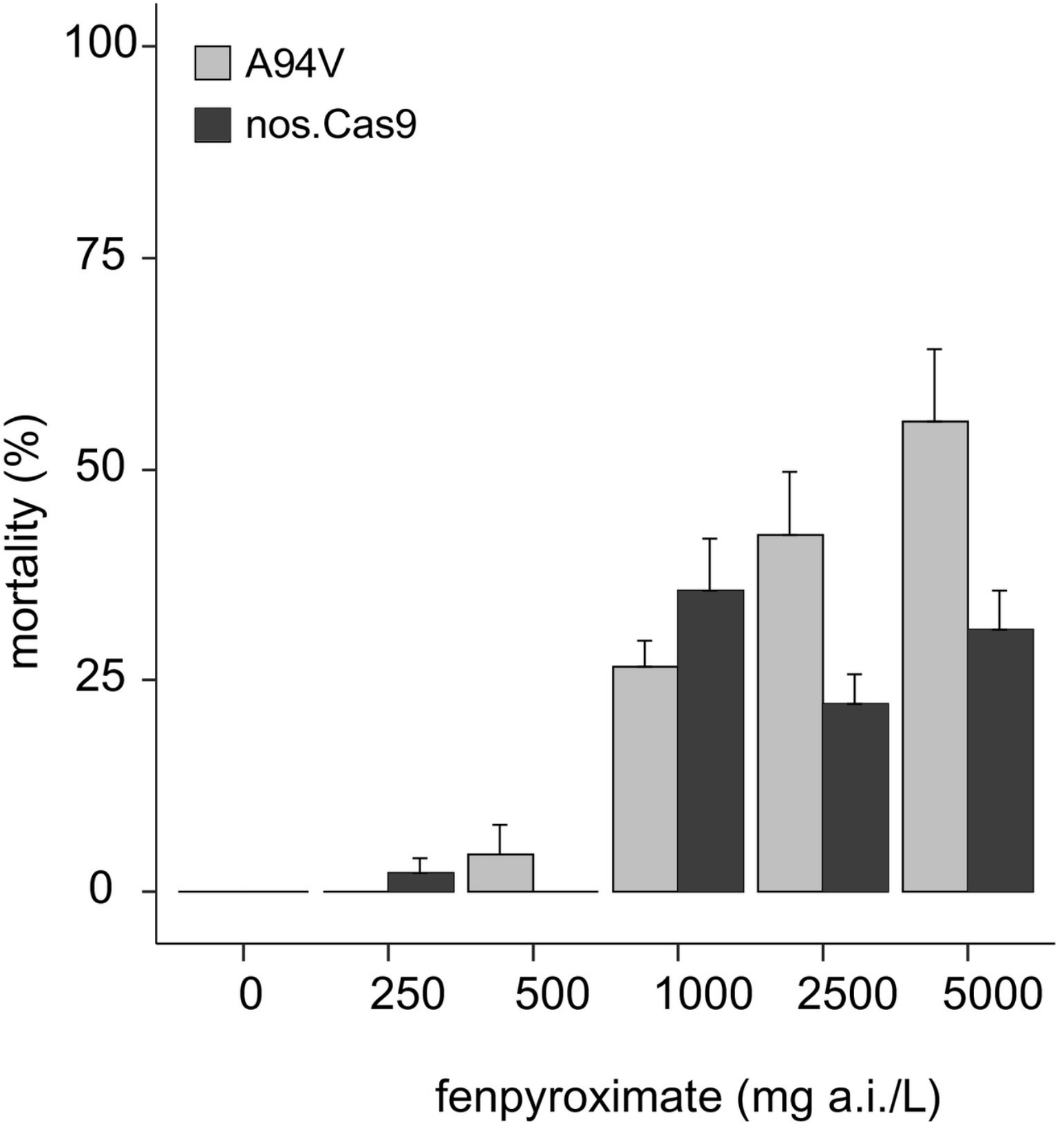
100
75
50
25
0
mortality (%)
A94V
nos.Cas9
0
250
500
1000
2500
5000
fenpyroximate (mg a.i./L)

Figure 3

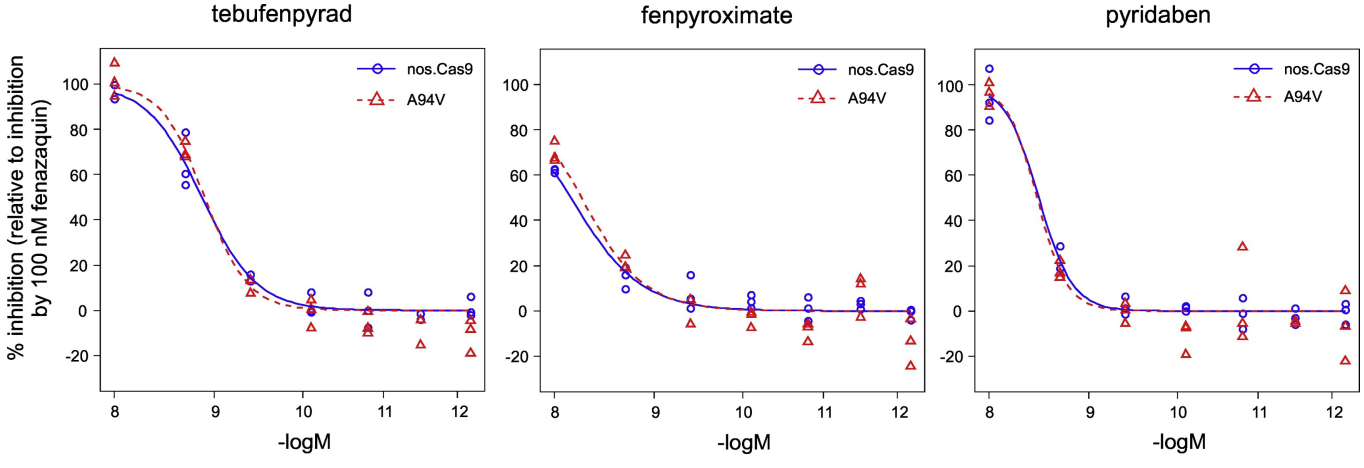
tebufenpyrad
fenpyroximate
pyridaben
% inhibition (relative to inhibition by 100 nM fenazaquin)
nos.Cas9
A94V
-logM
100
80
60
40
20
0
-20
8
9
10
11
12

Figure 4

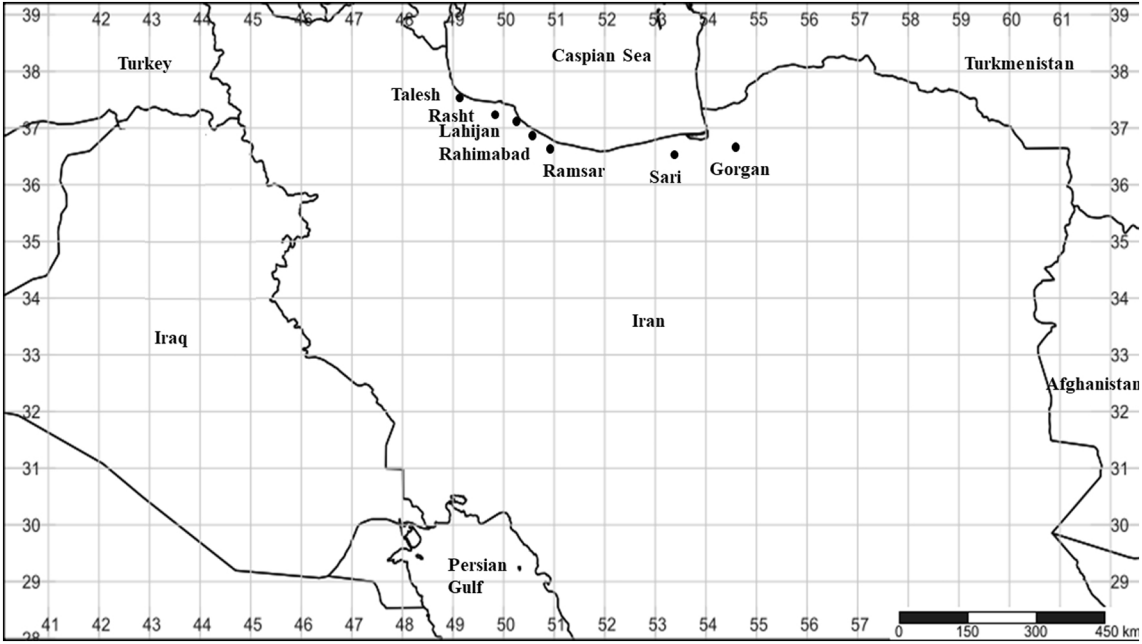
Turkey
Caspian Sea
Turkmenistan
Talesh
Rasht
Lahijan
Rahimabad
Ramsar
Sari
Gorgan
Iraq
Iran
Afghanistan
Persian
Gulf
0 150 300 450 km

Figure 5

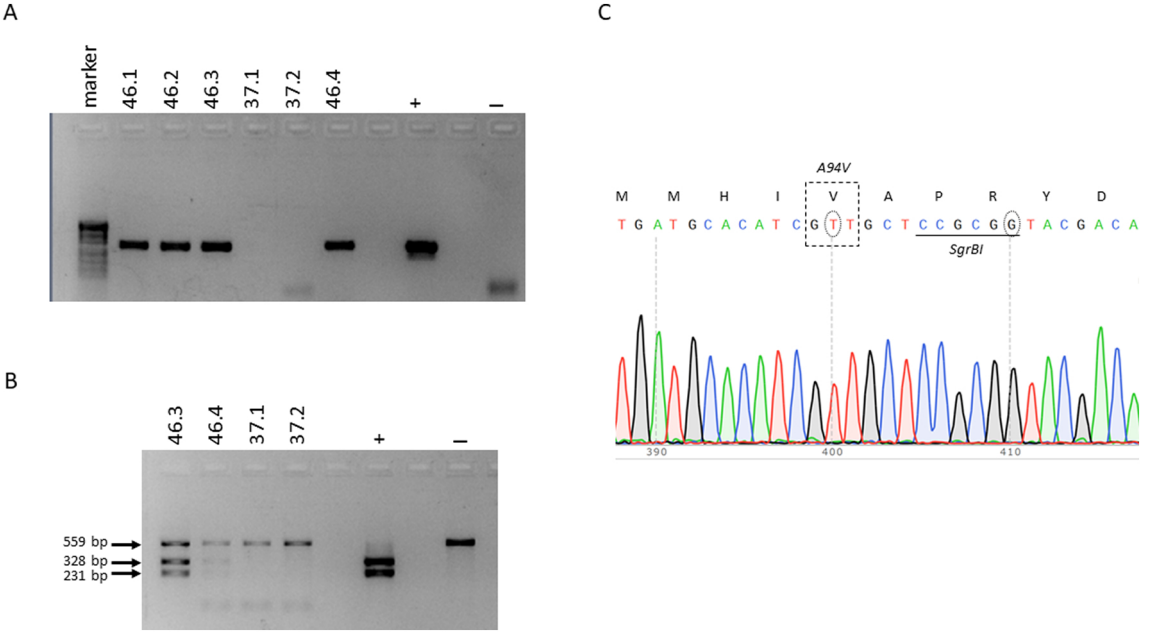
A
marker
46.1
46.2
46.3
37.1
37.2
46.4
+
–
B
46.3
46.4
37.1
37.2
+
–
559 bp
328 bp
231 bp
C
A94V
M M H I V A P R Y D
T G A T G C A C A T C G T T G C T C C G C G G T A C G A C A
SgrBI
390
400
410

Figure 6

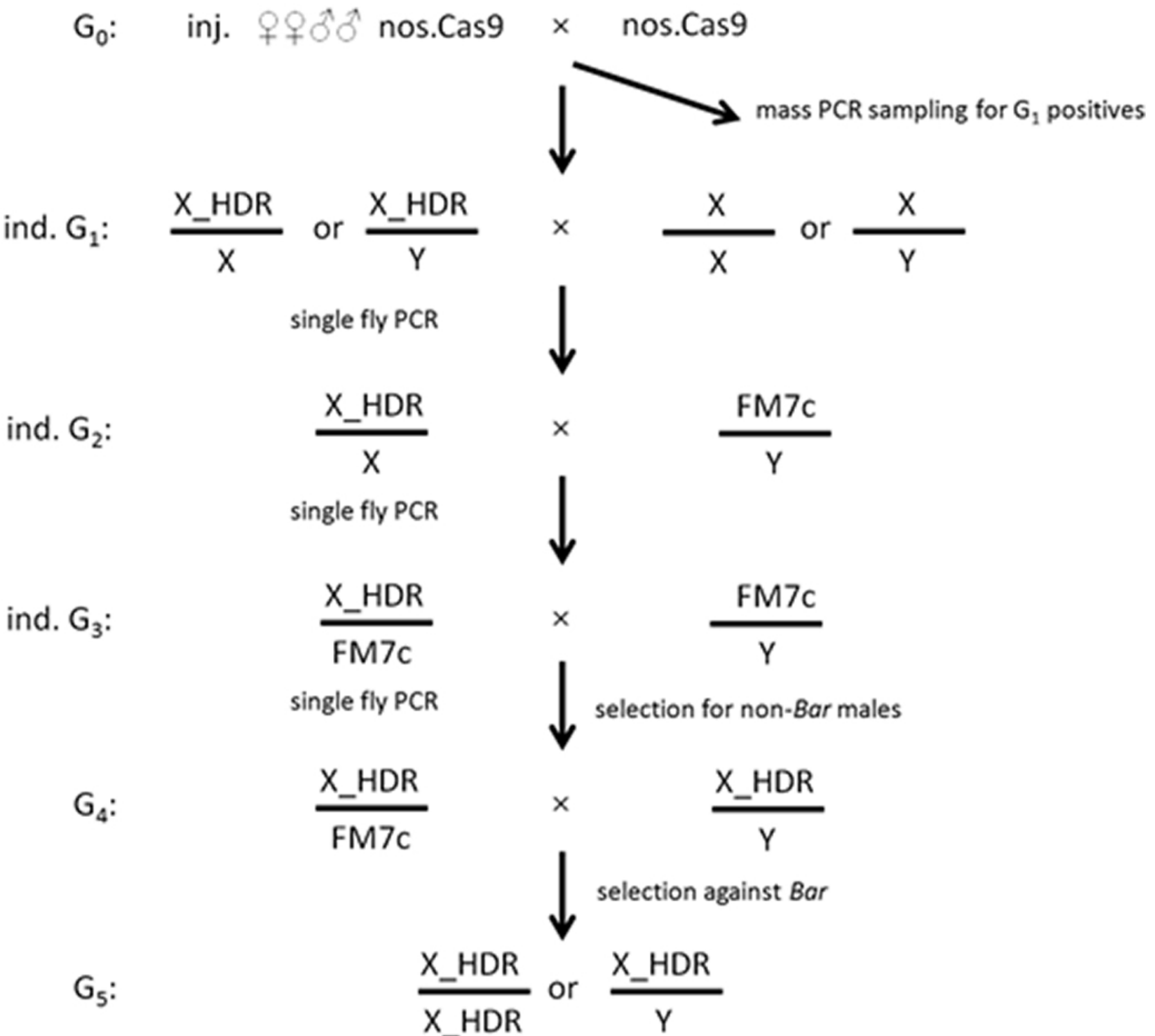
G0: inj. ♀♀♂♂ nos.Cas9 × nos.Cas9
mass PCR sampling for G1 positives
ind. G1: X_HDR / X or X_HDR / Y × X / X or X / Y
single fly PCR
ind. G2: X_HDR / X × FM7c / Y
single fly PCR
ind. G3: X_HDR / FM7c × FM7c / Y
single fly PCR
selection for non-Bar males
G4: X_HDR / FM7c × X_HDR / Y
selection against Bar
G5: X_HDR / X_HDR or X_HDR / Y

Figure 7

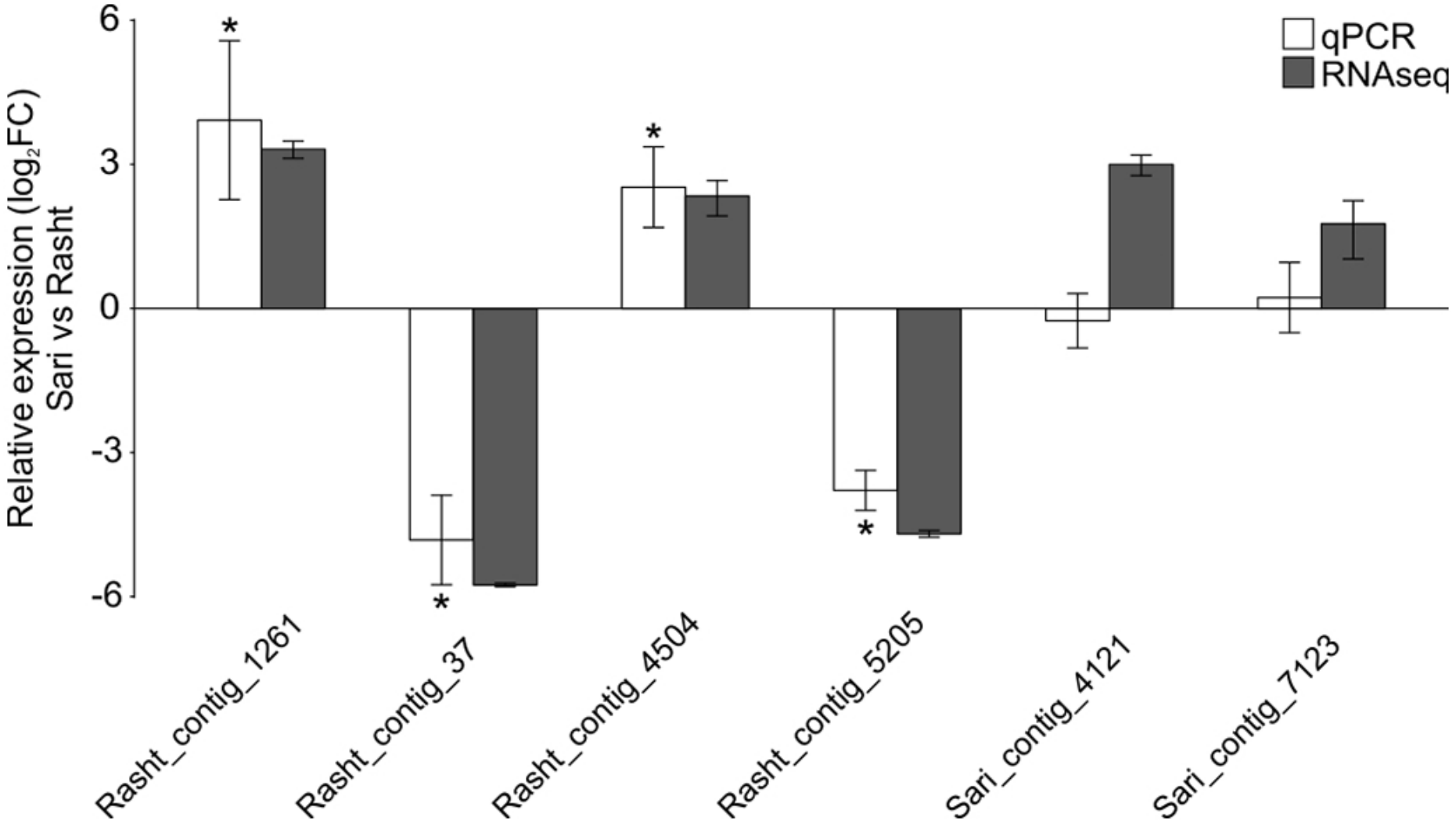
qPCR
RNAseq
Relative expression (log2FC)
Sari vs Rasht
6
3
0
-3
-6
*
*
*
*
Rasht_contig_1261
Rasht_contig_37
Rasht_contig_4504
Rasht_contig_5205
Sari_contig_4121
Sari_contig_7123

Figure 8

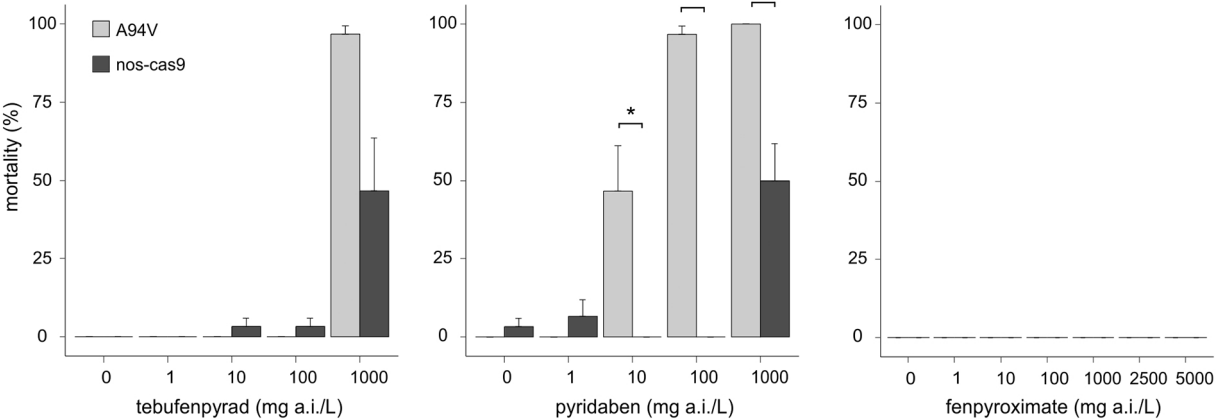
A94V
nos-cas9
mortality (%)
100
75
50
25
0
0
1
10
100
1000
tebufenpyrad (mg a.i./L)
*
*
*
pyridaben (mg a.i./L)
2500
5000
fenpyroximate (mg a.i./L)

Figure 9